Membrane Binding and Translocation of Cell-Penetrating Peptides†

Per E. G. Thorén,*,‡ Daniel Persson,‡ Elin K. Esbjörner,‡ Mattias Goksör,§ Per Lincoln,‡ and Bengt Nordén‡

Department of Chemistry and Bioscience, Chalmers University of Technology, SE-412 96 Gothenburg, Sweden, and Department of Experimental Physics, Chalmers University of Technology, SE-412 96 Gothenburg, Sweden

Received November 10, 2003; Revised Manuscript Received January 16, 2004

ABSTRACT: Cell-penetrating peptides (CPPs) have been extensively studied during the past decade, because of their ability to promote the cellular uptake of various cargo molecules, e.g., oligonucleotides and proteins. In a recent study of the uptake of several analogues of penetratin, Tat(48−60) and oligoarginine in live (unfixed) cells [Thorén et al. (2003) *Biochem. Biophys. Res. Commun. 307*, 100−107], it was found that both endocytotic and nonendocytotic uptake pathways are involved in the internalization of these CPPs. In the present study, the membrane interactions of some of these novel peptides, all containing a tryptophan residue to facilitate spectroscopic studies, are investigated. The peptides exhibit a strong affinity for large unilamellar vesicles (LUVs) containing zwitterionic and anionic lipids, with binding constants decreasing in the order penetratin > R_7W > TatP59W > TatLysP59W. Quenching studies using the aqueous quencher acrylamide and brominated lipids indicate that the tryptophan residues of the peptides are buried to a similar extent into the membrane, with an average insertion depth of ∼10−11 Å from the bilayer center. The membrane topology of the peptides was investigated using an assay based on resonance energy transfer between tryptophan and a fluorescently labeled lysophospholipid, lysoMC, distributed asymmetrically in the membranes of LUVs. By determination of the energy transfer efficiency when peptide was added to vesicles with lysoMC present exclusively in the inner leaflet, it was shown that none of the peptides investigated is able to translocate across the lipid membranes of LUVs. By contrast, confocal laser scanning microscopy studies on carboxyfluorescein-labeled peptides showed that all of the peptides rapidly traverse the membranes of giant unilamellar vesicles (GUVs). The choice of model system is thus crucial for the conclusions about the ability of CPPs to translocate across lipid membranes. Under the conditions used in the present study, peptide-lipid interactions alone cannot explain the different cellular uptake characteristics exhibited by these peptides.

The promising prospect of using oligonucleotides and polypeptides for therapeutic applications has made the delivery of large and hydrophilic molecules to the cytoplasm and nucleus of cells an increasingly important issue. Due to the barrier properties of the plasma membrane, the cellular uptake of such molecules is inherently poor, necessitating the development of efficient delivery vectors. In recent years, cell-penetrating peptides (CPPs[1]), also denoted protein transduction domains, have been widely used as carriers of a range of compounds (*1*−*4*). Members of this interesting class of peptides include penetratin, which constitutes the third helix of the Antennapedia homeodomain (*5*, *6*), Tat(48−60), derived from the HIV-1 Tat protein (*7*, *8*), and oligoarginines (*9*−*11*). The common properties of CPPs have been reported to be a rapid, energy-independent, and apparently nonendocytotic uptake, independent of cell-type, even when conjugated to cargo molecules such as oligonucleotides and polypeptides (*1*−*4*). This implies a yet unknown mechanism of uptake, possibly taking place via direct interaction with the membrane lipids. A model in which penetratin enters cells via the formation of inverted micelles within the plasma membrane has been suggested (*6*), and a similar uptake route has also been proposed for the Tat peptide (*7*). In search of an understanding of the physicochemical properties of CPPs, peptide−lipid interactions in lipid model systems have been studied. Especially penetratin, the two tryptophan residues of which enable fluorescence spectroscopy studies, has been thoroughly investigated (*12*−*24*). Although translocation of penetratin across a protein-free lipid bilayer was reported (*13*), the mechanism of cellular uptake has remained a puzzle.

† Supported by the Strategic Nucleic Acid Research Program and the Swedish Research Council.

* Corresponding author. Fax: +46-31-7723858. E-mail: thoren@phc.chalmers.se.

‡ Department of Chemistry and Bioscience.

§ Department of Experimental Physics.

[1] Abbreviations: CD, circular dichroism; CPP, cell-penetrating peptide; DA, distribution analysis; DFQP, depth-dependent fluorescence quenching profiles; DOPC, 1,2-dioleoyl-*sn*-glycero-3-phosphocoline; DOPG, 1,2-dioleoyl-*sn*-glycero-3-phosphoglycerol; DSPE-PEG(2000), 1,2-distearoyl-*sn*-glycero-3-phosphoethanolamine-N-[poly(ethylene glycol)2000]; EDTA, ethylenediaminetetraacetic acid; EggPC, egg phosphatidylcholine; FAB-MS, Fast atom bombardment mass spectrometry; FTIR, Fourier transform infrared spectroscopy; GUVs, giant unilamellar vesicles; HEPES, N-(2-hydroxyethyl)-piperazine-N′-(2-ethanesulfonic acid); HPLC, high-performance liquid chromatography; LysoPE, 1-palmitoyl-2-hydroxy-*sn*-glycero-3-phosphoethanolamine; LysoMC, (N-7-hydroxy-4-methylcoumarin-3-acetyl)-1-palmitoyl-2-hydroxy-*sn*-glycer o-3-phosphoethanolamine; LUVs, large unilamellar vesicles; methylcoumarin, 7-hydroxy-4-methylcoumarin-3-acetic acid; MLVs, multilamellar vesicles; NBD-PE, N-(7-nitrobenz-2-oxa-1,3-diazol-4-yl)-1,2-dipalmitoyl-*sn*-glycero-3-phosph oethanolamine; PM, parallax method; POPC, 1-palmitoyl-2-oleoyl-*sn*-glycero-3-RET, resonance energy transfer; ROI, region of interest; SbPC, soybean phosphatidylcholine; SVD, singular value decomposition; TOE, tryptophan octyl ester.

10.1021/bi0360049 CCC: $27.50
Published on Web 03/02/2004

Recently, it was shown that cell fixation, commonly used for studies of the intracellular localization of fluorophore-labeled compounds, leads to an artificial uptake of peptide associated with the plasma membrane (*25*, *26*). Likewise, the results of flow cytometry analysis, which is also frequently employed in studies of cellular uptake, can be misinterpreted if one does not consider that the measured fluorescence intensity stems from the entire cells, including the outside of the plasma membranes (*25*, *26*). Since CPPs are typically highly basic peptides with a high affinity for the cell surface, a substantial amount of peptide added to cells will remain associated with the plasma membranes even after extensive washing with buffer (*26*). Unfortunately, most of the studies of CPPs found in the literature are based on cell studies using fixed cells and/or flow cytometry analysis and may thus be prone to artifacts as described above, calling for a reevaluation of most findings fundamental for our understanding of CPPs. Future cell studies should therefore be performed using live (unfixed) cells.

In live CHO and HeLa cells, uptake via endocytosis has now been reported for Tat(48-60) and oligoarginine (*26*), and similar observations were also made for VP22, another CPP (*25*). In a live cell study published recently, we compared the cellular uptake of carboxyfluorescein-labeled penetratin and some of its analogues with that of oligoarginine and Tat in V79 and PC-12 cells (*27*). In the Tat-(48−60) and heptaarginine analogues, denoted TatP59W and R_7W, respectively, a tryptophan residue was inserted in order to be able to take advantage of the useful spectroscopic properties of tryptophan for a comparison of the same peptides in lipid model systems, without the carboxyfluorescein tag. Penetratin was apparently internalized via endocytosis, since incubation at low temperature or with depletion of intracellular ATP inhibited the cellular uptake of the peptide. For R_7W, cell internalization was not inhibited under such conditions, suggesting a different, energy-independent uptake mechanism. TatP59W exhibited internalization properties somewhere between those of penetratin and R_7W, in that its cellular uptake was inhibited by depletion of intracellular ATP, but not by incubation at low temperature. This suggests that competing uptake pathways are involved. Strikingly, TatLysP59W, an analogue in which the arginine residues of Tat were substituted for lysines, was not internalized at all. In fact, it exhibited a very low overall affinity for the cell surface, contrary to the parent peptide TatP59W. The same observation was made for arginine-to-lysine substitution in penetratin, indicating a key role for the arginine residues in the cellular uptake of CPPs, as proposed earlier (*9*, *11*).

Uptake via endocytosis has been considered undesirable for the delivery of gene-targeted drugs, leading to entrapment of drug molecules in endosomal vesicles and subsequent degradation (*28*). Nevertheless, there are numerous examples where CPPs have been successfully employed to deliver oligonucleotides, PNAs, and polypeptides to the cytoplasm and nucleus of live cells, leading to a biological response (see refs *29*−*31* and references therein). Thus, although it is obvious from live cell studies that endocytosis plays a significant role in the internalization of at least some of the CPPs, the fate of internalized cargo molecules is not limited to endosomal compartments. One could speculate that some CPPs act by mediating the escape of conjugated moieties from endosomal vesicles. Furthermore, at least for oligoarginines, live cell studies suggest that an uptake pathway not involving endocytosis may be predominant (*9*, *27*). In neither case, the mechanisms by which CPPs aid the delivery of hydrophilic macromolecules are fully understood. Studies of peptide−lipid interactions in model systems can thus give valuable clues.

Table 1: Names and Amino Acid Sequences of Peptides Studied in This Work[a]

name	sequence
penetratin	Ac-RQIKIWFQNRRMKWKK-NH_2
TatP59W	Ac-GRKKRRQRRRPWQ-NH_2
TatLysP59W	Ac-GKKKKKQKKKPWQ-NH_2
R_7W	Ac-RRRRRRRW-NH_2
Ac-18A-NH_2	Ac-DWLKAFYDKVAEKLKEAF-NH_2

[a] Peptides used for confocal microscopy studies were not capped in the N-terminus. Instead, they were conjugated to carboxyfluorescein.

In the present study, the interactions of penetratin, R_7W, TatP59W, and TatLysP59W (Table 1) with phospholipid vesicles have been investigated. As discussed above, these peptides exhibit vastly different uptake characteristics in live cells (*27*), ranging from endocytotic uptake (penetratin) to nonendocytotic (R_7W) or no uptake at all (TatLysP59W). First, the binding of the peptides to negatively charged vesicles was investigated and quantified using fluorescence spectroscopy. Knowledge of the extent of binding is of vital importance for the design of experiments as well as a proper interpretation of the results. Furthermore, large differences in affinity for the cell surface were observed for TatP59W and TatLysP59W (*27*), making a comparison of the extent of membrane association of these peptides particularly interesting. Due to the propensity of the CPPs investigated to induce vesicle aggregation, vesicles containing 5 mol % of poly(ethylene glycol)-conjugated lipid (DSPE-PEG) were used. The inclusion of DSPE-PEG was found to prevent peptide-induced vesicle aggregation, which would otherwise drastically increase the optical density of the sample and thus severely disturb the measured fluorescence signal. The peptides exhibited a strong affinity for vesicles containing the zwitterionic lipid dioleoylphosphatidylcholine (DOPC) and the negatively charged lipid dioleoylphosphatidylglycerol (DOPG). The binding data were analyzed according to a model based on the Gouy−Chapman theory in combination with a two-state surface partition equilibrium, separating the electrostatic and the hydrophobic contributions to the binding free energy (*32*). To further characterize the interaction of the peptides with lipid bilayers, the depth of membrane insertion was investigated, using the aqueous quencher acrylamide as well as brominated lipids for the quenching of tryptophan fluorescence. The results indicated that the tryptophan residues of the CPPs investigated penetrate to a similar extent into the lipid bilayers of vesicles composed of DOPC/DOPG (60/40). The calculated penetration depth of the tryptophan residues was ∼10−11 Å from the bilayer center for all the peptides. A key question for the understanding of the mechanism of internalization in cells is whether the peptides are able to translocate across protein-free lipid membranes. This important issue was addressed using two different types of lipid model systems: large unilamellar vesicles (LUVs), prepared by extrusion, and giant unilamellar vesicles (GUVs). For the study of peptide

translocation in LUVs (~100 nm in diameter), a method based on resonance energy transfer between tryptophan residues and a lipid-anchored probe was employed. The assay used here is a variant of a recently proposed method using methylcoumarin conjugated to lysophosphatidylethanolamine, lysoMC (*33*), using vesicles with the probe exclusively located in the inner leaflet of the lipid bilayer. The extent of energy transfer from tryptophan in the exogenously added CPPs to lysoMC-labeled vesicles was compared with that of two reference compounds: tryptophan octyl ester, known to readily equilibrate across lipid bilayers, and the nontranslocating peptide Ac-18A-NH_2. None of the CPPs examined were able to translocate across the membranes of the smaller vesicles (LUVs) for any of the lipid compositions tested. However, the opposite result was obtained for giant vesicles, several microns in diameter: when carboxyfluorescein-labeled peptides were added to GUVs sitting on a coverslip, translocation to the interior of the vesicles was observed for penetratin, R_7W, TatP59W, and TatLysP59W by use of confocal laser scanning microscopy. Our study thus indicates that the translocation properties of a peptide may depend sensitively on the membrane model system. The implications for the mechanism of uptake of the peptides investigated are discussed.

MATERIALS AND METHODS

Materials. 1,2-Dioleoyl-*sn*-glycero-3-phosphocoline (DOPC) and egg phosphatidylcholine (EggPC) were purchased from Larodan. 1,2-Dioleoyl-*sn*-glycero-3-phosphoglycerol (DOPG), tryptophan octyl ester (TOE), poly(ethyleneimine) [50% (w/v) aqueous solution], and melittin were obtained from Sigma. 1-Palmitoyl-2-stearoyl(6−7, 9−10, and 11−12)-dibromo-*sn*-glycero-3-phosphocholine (6−7-diBrPC, 9−10-diBrPC and 11−12-diBrPC) was obtained from Avanti Polar Lipids. 1,2-Distearoyl-*sn*-glycero-3-phosphoethanolamine-N-[poly(ethylene glycol)2000] (DSPE-PEG) was from BioTrend. Polar lipid extract of soybean lecithin, consisting of a mixture of phosphatidylcholine (45.7%), phosphatidylethanolamine (22.1%), phosphatidylinositol (18.4%), phosphatidic acid (6.9%), and others (6.9%), was obtained from Avanti Polar Lipids. Soybean phosphatidylcholine (Epikuron 200) was obtained from Lucas Meyer. N-(7-Nitrobenz-2-oxa-1,3-diazol-4-yl)-1,2-dipalmitoyl-*sn*-glycero-3-phosphoethan olamine (NBD-PE), 7-hydroxy-4-methylcoumarin-3-acetic acid succinimidyl ester, and 5-(and-6)-carboxyfluorescein succinimidyl ester were purchased from Molecular Probes. L-Tryptophan was from Merck. Oligonucleotide (GTAGATCACTGTAGTACACT), labeled with fluorescein in the 5′ end, was from MedProbe. Ac-18A-NH_2 (18 residue amphipathic class A peptide) was obtained from K J Ross Pedersen AS. Standard Fmoc-protected amino acids were obtained from Nova Biochem (Arg, Lys, Met, Trp, Phe), Alexis Corporation (Gln, Asn) and Perseptive Biosystems (Ile). In all fluorescence experiments except the study on giant vesicles (vide infra), the buffer used was 10 mM HEPES, 5 mM NaOH, 1 mM EDTA, and 0.1 M NaCl (pH 7.4). Deionized water from a Milli-Q system (Millipore) was used. For circular dichroism measurements, a 5 mM sodium phosphate buffer (pH 7.4) was used.

Peptide Synthesis. Peptides (penetratin, TatP59W, TatLysP59W, and R_7W) were synthesized on a Pioneer Peptide synthesizer (Perseptive Biosystems). Fmoc solid-phase synthesis was carried out on an Fmoc-PAL-PEG-PS support, resulting in an amidated carboxyl terminus after cleavage from the resin. After the synthesis was complete, peptides used for spectroscopic studies were capped with an acetyl group at the amino terminus. In the case of carboxyfluorescein-labeled peptides, this end was left open for labeling with carboxyfluorescein. For the labeling reaction, a 1-fold excess of carboxyfluorescein succinimidyl ester was added along with resin-bound peptide to dimethylformamide, and the reaction container was subjected to 24 h of gentle shaking. Penetratin was cleaved from the resin with trifluoroacetic acid:1,2-ethanedithiol:water:triisopropylsilane (94:2.5:2.5:1) for 2 h. For the Tat analogues and R_7W, a solution of trifluoroacetic acid:water:triisopropysilane (95:2.5:2.5) and a cleavage time of 4 h was used. After precipitation by addition of cold ether, the peptides were collected by centrifugation, washed twice with ether, dried, dissolved in water, and lyophilized. Preparative reversed-phase HPLC (Kromasil C8 column, Eka Chemicals) was used to further purify the peptides (isocratic elution: water/trifluoroacetic acid/2-propanol or water/trifluoroacetic acid/acetonitril). Peptide concentrations in aqueous solutions were determined by UV absorbance at 280 nm, using a molar extinction coefficient for tryptophan of 5690 M^{-1} cm^{-1} (*34*). Stock solution concentrations were found to correspond to ~70−80% of the weighed amount of peptide, which was the basis for calculation of peptide concentrations in our previous study of the membrane binding of penetratin (*15*).

Synthesis of LysoMC. LysoMC, N-(7-hydroxy-4-methylcoumarin-3-acetyl)-1-palmitoyl-2-hydroxy-*sn*-glycero-3-p hosphoethanolamine, was synthesized by reacting 7-hydroxy-4-methylcoumarin-3-acetyl-succinimidyl ester with 1-palmitoyl-2-hydroxy-*sn*-glycero-3-phosphoethanolamine (lysoPE) (Alexis). A 20 mg sample of the probe was incubated with two equivalents of DIPEA and 20 mg of the lysolipid in 1.8 mL methanol in an Eppendorff tube for 24 h at room temperature. The product was purified by preparative reversed-phase HPLC (Kromasil C8 column, Eka Chemicals), using a 40 min gradient of 5−70% acetonitrile in acetate buffer (pH 6). The identity of the fluorescently labeled lipid was confirmed by FAB-MS and the purity further confirmed by analytical thin-layer chromatography. After purification, the product was lyophilized and stored at −20 °C. The reaction yield was approximately 60% with respect to lysoPE. For preparation lysoMC-labeled vesicles, a stock solution of lysoMC dissolved in chloroform containing 1% methanol was used.

Prevention of Peptide Adsorption during Fluorescence Spectroscopy Studies. We recently showed that adsorption of penetratin to cuvette walls, standard propylene pipet tips and to Teflon magnetic stirrer bars can lead to serious errors in spectroscopic measurements (*15*). We have now also observed substantial adsorption to quartz cuvette walls for the Tat peptides and R_7W used in this work (data not shown). Adsorption to plastic and glass was also observed by Chico et al. for penetratin and Tat(48−60) (*35*). As was shown in ref *15*, adsorption of the positively charged peptide penetratin can be prevented by preadsorption of poly(ethyleneimine), a cationic polymer, to the surface of the interior cuvette walls. The use of poly(ethyleneimine) proved to be very effective also for the prevention of adsorption of R_7W, TatP59W, and TatLysP59W (data not shown). Modification of the surface

of the interior cuvette walls was accomplished by leaving the cuvette filled with a 1% (w/v) solution of poly(ethyleneimine) in deionized water for 30 min, followed by thorough rinsing with deionized water. The polymer is not desorbed by repeated washings with aqueous solutions.

Preparation of Large Unilamellar Vesicles (LUVs). Chloroform solutions of lipid were mixed to obtain the desired ratio of zwitterionic and negatively charged lipids, and the solvent was removed under reduced pressure with a rotary evaporator. The dry phospholipid film was placed in high vacuum for 2 h to remove trace amounts of chloroform. Vesicles were prepared by dispersion of the lipid film in buffer. The dispersion was subjected to five freeze−thaw cycles (*36*) before extrusion 21 times through two 100 nm polycarbonate filters on a LiposoFast-Pneumatic extruder (Avestin, Canada) to obtain large unilamellar vesicles (LUVs). The lipid concentration was determined by the Stewart assay (*37*). A homogeneous liposome size distribution around 100 nm was confirmed by dynamic light scattering analysis, using a Malvern Instrument Series 7032 Multi-8 correlator and a PCS100 spectrometer (Malvern Instruments).

Circular Dichroism. Circular dichroism (CD) was measured on a Jasco J-810 spectropolarimeter using a 1 mm quartz cell. All spectra were taken between 190 and 260 nm and corrected for background contributions. Peptide concentrations were 5 μM, and the lipid concentration was 500 μM. Results are expressed as mean residue ellipticities $[\theta]_{MR}$ (deg cm^2/dmol). Reference CD spectra used for comparison of the acquired spectra were taken from Perczel et al. (*38*).

Fluorescence. Fluorescence was measured on a Spex Fluorolog τ-3 spectrofluorometer (JY Horiba) using a 1 × 1 cm quartz cell thermostated at 25.0 °C. The band-pass of the excitation slit was adjusted to obtain an optimal signal-to-noise ratio without photodegradation.

Binding Experiments. A solution containing large unilamellar vesicles (50 μM lipid concentration) was titrated with microliter aliquots of peptide stock solution (100 μM). After each addition of peptide, a spectrum was recorded between 315 and 400 nm with an increment of 1 nm and an integration time of 2 s, using an excitation wavelength of 280 nm. The spectra were corrected for buffer and liposome background. Several titrations were performed for each peptide and used together for the construction of binding isotherms. The spectral data was analyzed using Matlab (The MathWorks Inc.). For singular value decomposition of the titration spectra (see Appendix, eq A1), the Matlab command *svd* was employed, and for least-squares projection of titration spectra on reference spectra (eq A3), the *pinv* command was used.

Acrylamide Quenching Experiments. For acrylamide quenching experiments (*39*), an excitation wavelength of 295 nm instead of 280 nm was used in order to reduce the effect of acrylamide absorbance (*40*). Aliquots of acrylamide were added from a 4 M stock solution to 1 μM of peptide in the absence or in the presence of DOPC/DOPG (60/40) vesicles, and the fluorescence at 350 nm was monitored after each addition. The data were corrected for dilution and vesicle background intensity and analyzed according to the Stern−Volmer equation (*41*):

$$\frac{F_0}{F} = 1 + K_{SV}[Q] \tag{1}$$

where F_0 and F are the fluorescence intensities in the absence and in the presence of quencher, respectively, [Q] is the molar concentration of quencher, and K_{SV} is the Stern−Volmer quenching constant. K_{SV} was calculated as the slope of the Stern−Volmer plot, which is linear for acrylamide concentrations up to 0.1 M (*40*, *42*).

Brominated Lipid Quenching Experiments. Depth-dependent fluorescence quenching of tryptophan was performed in LUVs composed of DOPC, DOPG, and either (6,7)-, (9,10)-, or (11,12)-BrPC at molar ratios of 30:40:30. BrPC-concentrations were determined by Fourier Transform Infrared (FTIR) spectroscopy on the carbonyl bonds (the carbonyl stretch vibration has an absorption band at 1740 cm^{-1}) using a Bruker IFS 66v/S FTIR spectrometer equipped with a nitrogen cooled MCT-detector. A sample cell with sodium chloride windows was used. All measurements were performed using lipids in chloroform solutions and spectra were corrected for chloroform background intensity. FTIR has proven to be a fast and reliable method for determination of phospholipid concentrations (Persson et al., unpublished experiments). Fluorescence intensities in absence of quencher (F_0) were measured in DOPC/DOPG (60/40) vesicles. Spectra were recorded between 315 and 400 nm with an increment of 1 nm and an integration time of 2 s, using an excitation wavelength of 280 nm. The peptide to lipid molar ratios were approximately 1:100, and peptide concentrations were 1 μM (for penetratin, melittin, TOE, and Ac-18A-NH$_2$) or 2 μM (for TatP59W, TatlysP59W, and R$_7$W). Data were corrected for vesicle background, and the total intensity was calculated as the sum of all measured points in each spectrum. Depth-dependent fluorescence quenching profiles (DFQPs) were fitted to data in Matlab using the distribution analysis (DA) method (*43*, *44*) as well as the parallax method (PM) (*45*−*47*)

$$\text{DA:} \quad \ln\frac{F_0}{F(h)} = \frac{S}{\sigma\sqrt{2\pi}}\exp\left[-\frac{(h-h_m)^2}{2\sigma^2}\right] \tag{2}$$

$$\text{PM:} \quad \ln\frac{F_0}{F(h)} = \pi C[R_c{}^2 - (h-h_m)^2] \; h - h_m < R_c$$

$$\ln\frac{F_0}{F(h)} = 0 \qquad h - h_m \geq R_c \tag{3}$$

In the equations above, F_0 is the fluorescence intensity in absence of quencher, $F(h)$ is the intensity in the presence of quencher at the distance h (Å) from the bilayer center, and h_m is the average insertion depth of the tryptophan residues. In DA the DFQP data are fitted with a Gaussian function where σ denotes the dispersion, which is related to the in-depth distribution of the tryptophan chromophores, and S is the area under the quenching profile, which is related to the quenchability of the tryptophan moiety. The parallax method fits data to a truncated parabola, and R_c is the radius of quenching (*44*, *48*−*50*). Even though the brominated lipids used contain no double bonds, they form bilayers of equal thickness to POPC (*51*), with a hydrocarbon core of ∼29 Å and a total bilayer thickness of ∼49 Å. The brominated lipids behave much like ordinary lipids with one unsaturated bond since the bulkiness of the bromine atoms have similar effects on lipid packing as a cis double bond (*52*). Wiener and White

(*53*) state that the carbonyl group can be thought of as a marker of the hydrocarbon/headgroup boundary and according to their measurements, a DOPC bilayer has a hydrocarbon core of approximately 30 Å. It is therefore reasonable to assume that the average bromine distances from the lipid bilayer center, as determined by McIntosh and Holloway (*51*), are valid also in the vesicles used in this study. Average bromine distances from the bilayer center (h) were thus taken to be 11.0, 8.3, and 6.5 Å for (6,7)-BrPC, (9,10)-BrPC and (11,12)-BrPC, respectively.

Asymmetric Labeling of LUVs. Large unilamellar vesicles with lysoMC present in the inner leaflet only can be prepared by removing lysoMC from the outer leaflet of symmetrically labeled LUVs. This is accomplished by mixing vesicles containing 1 mol % lysoMC symmetrically distributed between the inner and the outer leaflet with an excess of large lipid particles, serving as acceptors for lysoMC lipids, which are water-soluble and readily redistribute between vesicles. After equilibration, the lysoMC vesicles (∼100 nm in diameter) are separated from the large lipid particles (several microns in diameter) by centrifugation.

Large lipid particles were prepared from soybean phosphatidylcholine (SbPC), which was dispersed in buffer at a concentration of 20 mg/mL by extensive vortexing. Examination of the dispersion by microscopy showed that it consisted predominantly of large lipid particles with an undefined structure (5−20 μm) and multilamellar vesicles, generally somewhat smaller in size (data not shown). Prior to mixing with the lysoMC vesicles, trace amounts of small lipid particles and liposomes, comparable to the lysoMC vesicles in size, were removed from the SbPC dispersion by centrifugation (5000*g*, 25 °C, 5 min). The supernatant was removed and replaced with buffer. The pellet was resuspended and centrifuged (50 000*g*, 25 °C, 15 min). The fluorescence of α-tocopherol, which is present in most soybean lipid extracts, was used as an indicator for the presence of small lipid particles and liposomes in the supernatant. After each centrifugation, the fluorescence intensity of the supernatant was measured using an excitation wavelength of 290 nm and an emission wavelength of 335 nm, to detect the presence of α-tocopherol. The cycle (resuspension of the pellet in fresh buffer followed by centrifugation) was repeated until a negligible fluorescence (<0,1% of the initial value) was detected in the supernatant.

Symmetrically labeled lysoMC vesicles at 2 mM concentration (1.5 mL) were added to SbPC pellets (∼30 mg per pellet) in Eppendorff tubes, and the pellets were resuspended. After equilibration for 15 min, the tubes were centrifuged (50 000*g*, 25 °C, 15 min). After centrifugation, the lysoMC fluorescence in a fraction of the supernatant was examined and compared to the fluorescence in the symmetrically labeled lysoMC vesicles. To distinguish the fraction of lysoMC present in the outer leaflet of the vesicles from the lysoMC located in the inner leaflet, sodium hydroxide was added to the surrounding solution, raising the external pH to 11. This results in an immediate decrease in the fluorescence intensity at 400 nm, as the methylcoumarin headgroup of the lysoMC molecules in the outer leaflet is deprotonated (see Results). With time, the fluorescence intensity decreases further, as hydroxide ions leak into the vesicle interior and lysoMC in the inner leaflet is deprotonated. The signal decrease immediately after addition of sodium hydroxide was therefore used as a measure of the fraction of lysoMC remaining in the outer leaflet. The supernatant was transferred to another Eppendorff tube containing an SbPC pellet, and a new cycle (resuspension of the pellet followed by equilibration for 15 min and separation by centrifugation) was initiated. The procedure was repeated until the decrease in fluorescence intensity of the supernatant upon raising the pH was minute, corresponding to ∼1% of the decrease observed in symmetrically labeled vesicles. This was considered to correspond to a negligible amount of lysoMC in the outer leaflet.

Vesicles with lysoMC present exclusively in the outer leaflet were prepared by adding an appropriate amount of lysoMC from a stock solution in buffer to lysoMC-free vesicles. LysoMC stock solutions were prepared by evaporation of a chloroform solution of lysoMC in a stream of inert gas. Trace amounts of chloroform were removed by placing the sample in high vacuum for 2 h. The lipid film was subsequently dissolved in buffer. LysoMC solutions were prepared and used the same day.

Determination of Peptide Translocation in LUVs. In two separate experiments, peptide or TOE was added from stock solution to vesicles either asymmetrically labeled with lysoMC (see above) or devoid of lysoMC. Spectra were recorded between 300 and 500 nm, using an excitation wavelength of 260 nm (in order to minimize direct excitation of lysoMC) and corrected for vesicle background. The contribution of the tail of the tryptophan emission spectrum to the measured emission spectrum was eliminated by subtracting the appropriate fraction of the tryptophan emission spectrum measured when bound to the lysoMC-free vesicles, thereby making the tryptophan emission peak vanish. The increase in lysoMC fluorescence due to resonance energy transfer from tryptophan was then calculated by comparing the lysoMC fluorescence intensity at 460 nm in the absence and in the presence of the tryptophan-containing compound.

Preparation of Giant Unilamellar Vesicles (GUVs). Giant vesicles were formed from a polar lipid extract of soybean lecithin (Avanti Polar Lipids), consisting of a mixture of phosphatidylcholine (45,7%), phosphatidylethanolamine (22,1%), phosphatidylinositol (18,4%), phosphatidic acid (6,9%), and others (6,9%). Giant unilamellar vesicles (GUVs) were prepared using a dehydration/rehydration technique (*54*, *55*). In short, a dry phospholipid film was prepared by rotary evaporation of a chloroform solution of lipid. The lipid film was swelled by careful addition of buffer solution (5 mM Tris, 10 mM K_3PO_4, 10 mM KH_2PO_4, 90 mM KCL, 1 mM $MgSO_4$, 0.5 mM EDTA, 1 mM NaN_3, pH 8.1) and left in a refrigerator overnight. Glycerol (1% v/v) was added to the solution, which was then placed in an ultrasonic bath for 15 min. 5 μL of the resulting lipid dispersion (1 mg/mL) was placed on a cover slip glass and the solution was dehydrated in a vacuum desiccator for 20 min. The dry lipid film was rehydrated with 0.5 mL buffer in order to swell the lipid film. Multilamellar vesicles (MLVs) as well as GUVs were formed within minutes.

Confocal Laser Scanning Microscopy. Peptide translocation across GUV membranes was assessed using a laser scanning confocal unit (MRC1024, BioRad) mounted on the side port of an inverted microscope (TE-300, Nikon). The dyes used in the experiment (carboxyfluorescein and fluo-

rescein) were excited using a fiber-coupled Ar laser (488 nm). The samples were imaged using a 40' Plan Fluor objective (Nikon) with a numerical aperture of 0.75. In combination with the applied confocal pinhole, this resulted in a depth of field (or longitudinal resolution) of 2 μm. A 522DF35 filter (emission 505−540 nm) was used. The signal was collected by using a 5 frame Kalman collection filter. Relative fluorescence was measured using LaserPix software (Bio-Rad).

RESULTS

Binding Isotherms. In our recent study of the uptake of a number of cell-penetrating peptides in live cells (*27*), we found large variations between the peptides regarding their affinity for the plasma membranes in the two cell lines tested. While penetratin, R_7W, and TatP59W all associated strongly with the cell membranes, TatLysP59W did not bind significantly to the cells, and was not internalized. To further investigate this finding, a comparative study of the binding of penetratin, TatP59W, TatLysP59W, and R_7W (Table 1) to a membrane model system (large unilamellar vesicles) was performed, using fluorescence spectroscopy. The membrane binding of peptides containing an intrinsic tryptophan residue is assessed from an increase in quantum yield and blue shift in emission wavelength accompanying the transfer of the indole chromophore from an aqueous environment to a nonpolar environment. In this way, we recently studied the membrane binding of penetratin to vesicles composed of the zwitterionic lipid dioleolyphosphatidylcholine (DOPC) and the anionic lipid dioleoylphosphatidylglycerol (DOPG) and found that the affinity of penetratin for the vesicle membranes was highly dependent on the fraction of negatively charged lipids in the membrane, reflecting the importance of electrostatic interactions between the peptide and the membrane (*15*). By inclusion of a tryptophan residue in R_7W, TatP59W, and TatLysP59W, a similar approach was possible here, though precautions had to be taken to circumvent artifacts from light scattering, which causes diminution of excitation light and an apparent shift in the emission spectrum (*56*). At elevated peptide to lipid molar ratios, penetratin has been shown to induce vesicle aggregation (*14*), which leads to a large increase in turbidity. For R_7W, TatP59W, and TatLysP59W, the peptide-induced vesicle aggregation is even more extensive than for penetratin and occurs at a much lower peptide-to-lipid ratio, obviating a proper binding analysis. Vesicle aggregation can, however, be prevented by incorporation of poly(ethylene glycol)−lipid conjugates (*57*), which provide steric hindrance for interbilayer contact. The presence of PEG_{2000} conjugated to distearoylphosphatidylethanolamine (DSPE-PEG) in vesicles composed of DOPC and DOPG has been shown to inhibit vesicle aggregation induced by the peptides examined here (Thorén et al., unpublished experiments). Vesicles containing 5% DSPE-PEG were thus used in this study of the membrane affinity of the peptides. The binding was monitored by titrating a solution containing liposomes with peptide stock solution and collecting a tryptophan emission spectrum at each point of the titration. Analysis of the binding data was performed as described previously (*15*). By projection of the titration spectra on membrane-bound and free peptide reference spectra, recorded in separate experiments (see Appendix), it was found that two species, free and bound peptide, within experimental errors, account for the spectral data (data not shown). This was the case for all peptides under investigation. The analysis thus yields the corresponding concentrations of free and membrane-bound peptide, denoted C_f and C_b, respectively (see Appendix). The membrane-bound peptide to lipid molar ratio, r, can then be calculated for each point of a titration:

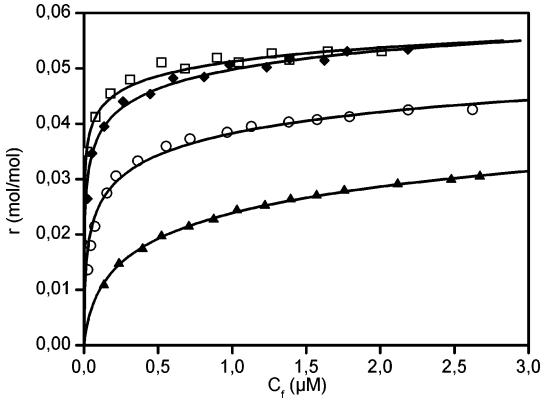

FIGURE 1: Binding isotherms for the association of penetratin (□), R_7W (◆), TatP59W (○), and TatLysP59W (▲) with DOPC/DOPG/DSPE-PEG (65/35/5) vesicles. The membrane-bound peptide to lipid molar ratio, *r*, is plotted against the free peptide concentration, C_f. The solid lines correspond to theoretical binding isotherms calculated according to a model combining the Gouy−Chapman equation theory with a surface partition equilibrium (see Discussion).

$$r = \frac{C_b}{L} \tag{4}$$

where *L* is the concentration of accessible lipid. Since the peptides associate exclusively with the outer leaflet of LUVs (vide infra), *L* was taken as 54% of the total lipid concentration, which corresponds to the theoretical fraction of lipid in the outer monolayer of spherical vesicles with a diameter of 100 nm, assuming a bilayer thickness of 4 nm. Figure 1 shows binding isotherms, *r* versus C_f, for penetratin, TatP59W, TatLysP59W, and R_7W for vesicles composed of DOPC/DOPG/DSPE-PEG (60/35/5). All four peptides exhibit a strong affinity for the vesicle membranes, decreasing in the order penetratin > R_7W > TatP59W > TatLysP59W. Inspection of the binding isotherms reveals that at a low degree of binding, the free peptide concentration is very low. This reflects a strong electrostatic attraction between the negatively charged membrane and the positively charged peptides (penetratin and R_7W formally carry seven positive charges and the Tat peptides carry eight positive charges). As is often observed for peptides carrying a net charge, there is a marked curvature with increasing *r*, reflecting the decreased electrostatic attraction between the peptide and the membrane as more and more peptide binds. The binding data were analyzed according to a model separating electrostatic and hydrophobic contributions to the binding free energy (see Discussion and Table 6).

Acrylamide Quenching. The access of the neutral, water-soluble quencher acrylamide to the tryptophan residues of penetratin, R_7W, TatP59W, and TatLysP59W at 1 μM concentration was examined in the absence and in the presence of vesicles. For penetratin, R_7W, and TatP59W, a lipid concentration of 200 μM was used. At this peptide to

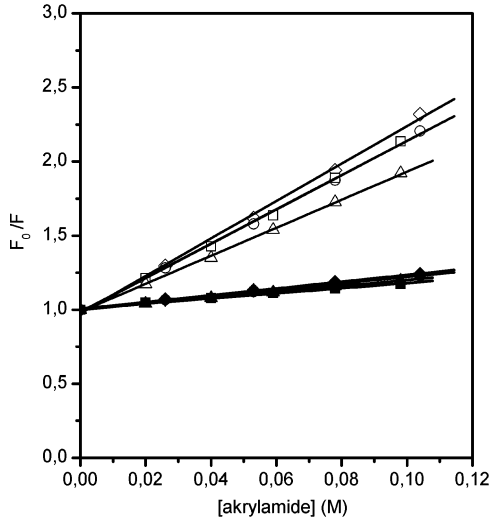

FIGURE 2: Stern−Volmer plots of fluorescence quenching of peptides by acrylamide in solution (open symbols) or in the presence of DOPC/DOPG (60/40) vesicles (closed symbols). Penetratin (■), R_7W (◆), TatP59W (●), and TatLysP59W (▲). The peptide concentration was 1 μM, and the lipid concentration was 200 μM for penetratin, R_7W, and TatP59W, and 400 μM for TatLysP59W.

Table 2: Tryptophan Emission Maxima and Stern−Volmer Quenching Constants (K_{SV}) for Peptides, TOE, and Free Tryptophan (Trp) at 1.0 μM Concentration in Buffer and in the Presence of DOPC/DOPG (60/40) Vesicles[a]

	buffer		DOPC/DOPG (60/40)		
peptide	λ_{max} (nm)[b]	K_{SV} (M^{-1})	λ_{max} (nm)	K_{SV} (M^{-1})	naf[c]
penetratin	350	11.6	337	1.7	0.15
R_7W	351	12.7	339	2.3	0.18
TatP59W	350	11.6	338	2.2	0.19
TatLysP59W	350	9.4	337	2.2	0.21
Ac-18A-NH_2	350	14.9	334	2.7	0.18
TOE[d]	354	15.0	333	1.8	0.12
Trp	351	16.3	351	16.5	1.01

[a] For TatLysP59W, a lipid concentration of 400 μM was used. For the other compounds, the lipid concentration was 200 μM. [b] Tryptophan emission maximum using an excitation wavelength of 295 nm. [c] Normalized accessibility factor, calculated as the ratio of K_{SV} in buffer and in the presence of vesicles. [d] Tryptophan octyl ester.

lipid molar ratio, the binding study presented above showed that the peptides effectively completely bound to the vesicles. For TatLysP59W, which showed a weaker affinity for the vesicles, a lipid concentration of 400 μM was used. Importantly, at the peptide to lipid molar ratios used, none of the peptides investigated induced vesicle aggregation (light scattering data not shown), which would otherwise influence the measured fluorescence intensities. Figure 2 shows Stern−Volmer plots of acrylamide quenching of penetratin, R_7W, TatP59W, and TatLysP59W in buffer and in the presence of DOPC/DOPG (60/40) vesicles. For comparison, the amphipathic class A peptide Ac-18A-NH_2 (Table 1), tryptophan octyl ester (TOE) and free tryptophan were also included in the study. The calculated Stern−Volmer quenching constants (K_{SV}, eq 1) for all the compounds investigated are summarized in Table 2. In buffer, the peptides all exhibit a tryptophan fluorescence maximum near 350 nm (Table 2), which is the maximum wavelength for free tryptophan, indicating that the tryptophan residues are fully exposed to the water solvent. In accordance with this, the tryptophan residues of the peptides examined were readily quenched by acrylamide, with a K_{SV} of 9−15 M^{-1}. In the presence of DOPC/DOPG (60/40) vesicles, the peptides and TOE exhibit a blue shift in tryptophan fluorescence, indicative of transfer of the tryptophan residue to the less polar environment of the vesicle membrane. A strong decrease in K_{SV} is observed for all of the peptides, as well as TOE, indicating that the tryptophan residues are more protected from the quencher acrylamide. To facilitate a comparison of the different peptides, a normalized accessibility factor (naf) was calculated as the ratio of the Stern−Volmer quenching constant in the presence of vesicles and the quenching constant in buffer (*40*). For R_7W, TatP59W, TatLysP59W, and Ac-18A-NH_2, a naf value of ~0.2 was obtained, while a slightly lower value was calculated for penetratin (Table 2). For free tryptophan, on the other hand, no change in the fluorescence emission maximum or K_{SV} is observed upon addition of vesicles, indicating that it does not interact with the vesicles to any appreciable extent in the concentration range used. For TOE, the reduction of the acrylamide quenching was larger than for the peptides examined.

Table 3: Quenching Efficiencies ($F(h)/F_0$) in Percent[a]

	peptide					
brominated lipid	penetratin	TatP59W	TatLys-P59W	R_7W	TOE	Ac-18A-NH_2
(6,7)-BrPC	64	61	65	56	73	63
(9,10)-BrPC	69	64	67	61	72	69
(11,12)-BrPC	83	79	82	78	87	82

[a] $F(h)$ is the tryptophan fluorescence intensity in vesicles containing lipids brominated at the level h, and F_0 is the tryptophan fluorescence intensity in the absence of quencher measured in DOPC:DOPG (60:40) vesicles.

Table 4: Average Insertion Depths Determined by the Distribution Analysis (DA) and Parallax Methods (PM), Together with the Respective Methods Fitting Parameters

	DA			PM-2	
peptide	h_m (Å)	σ (Å)	S	h_m (Å)	R_c (Å)
penetratin	10. 2	2.7	3.2	10.9	5.8
TatP59W	9.9	2.7	3.6	10.9	6.2
TatLysP59W	9.9	2.5	3.0	10.7	5.8
R_7W	10. 1	2.7	4.1	11.3	6.6
TOE	9.6	2.1	2.1	10.2	5.0
Ac-18A-NH_2	10. 3	2.9	3.5	10.9	5.9

Quenching by Brominated Lipids. The membrane insertion depth of the tryptophan residues in penetratin, TatP59W, TatLysP59W, and R_7W was examined and compared to the tryptophan depth in TOE and Ac-18A-NH_2 (used as reference compounds in the translocation studies). Depth-dependent fluorescence quenching data are presented in Table 3 as percentage of the fluorescence intensity in DOPC/ DOPG (60/40) vesicles. All investigated peptides exhibit comparable quenching patterns with most pronounced quenching in (6,7)-BrPC vesicles, whereas TOE shows similar degrees of quenching in (6,7)- and (9,10)-vesicles. Table 4 shows the determined average membrane insertion depth (h_m) presented as the distance from the bilayer center of the tryptophan residues in each peptide calculated using the distribution analysis and parallax methods (se Materials and Methods). Included in Table 4 are also the fitting parameters for both methods. Figure 3 exemplifies graphically the fitting to data by showing the depth-dependent quenching profiles for

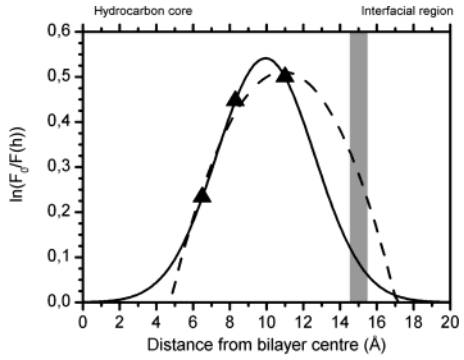

FIGURE 3: Depth-dependent quenching profiles of TatP59W, fitted to data using the distribution analysis (solid line) and parallax (dashed line) methods. The boundary between the hydrocarbon core region and the interfacial region of the bilayer is indicated by the gray area.

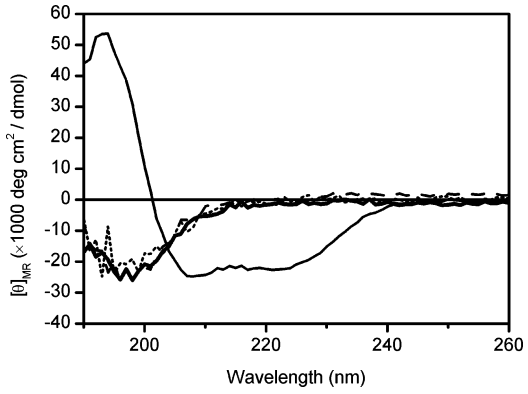

FIGURE 4: Circular dichroism spectra of penetratin (solid line), R_7W (dashed line), TatP59W (solid bold line), and TatLysP59W (dotted line) in the presence of DOPC/ DOPG/DSPE-PEG (65/35/5) vesicles at a peptide to lipid molar ratio of 1:100.

TatP59W as derived by DA and PM. The difference in membrane insertion depth computed by the two methods is small, typically ~1 Å or less. All peptides have an average tryptophan insertion depth of 10−11 Å, whereas the tryptophan moiety in TOE seems to be inserted somewhat deeper. The same measurements were also performed with the cationic hemolytic peptide melittin (GIGAVLKVLTTGLPALISWIKRKRQQ-NH_2), the tryptophan insertion depth of which has been extensively investigated earlier (*48*, *49*, *58*−*60*). Fitting of the data with DA and PM yielded average membrane insertion depths of 10.2 and 10.9 Å respectively.

Peptide Conformation. The secondary structure of penetratin, R_7W, TatP59W, and TatLysP59W in buffer and bound to DOPC/DOPG/DSPE-PEG (60/35/5) vesicles was investigated by circular dichroism. In buffer, all peptides were found to adopt a random coil conformation (data not shown). Figure 4 shows the circular dichroism spectra of the peptides in the presence of DOPC/ DOPG/DSPE-PEG (60/35/5) vesicles at a peptide to lipid molar ratio of 1:100. Penetratin has a circular dichroism spectrum characteristic of an α-helix, in line with our previous findings for penetratin bound to DOPC/DOPG vesicles at low peptide to lipid molar ratios (*15*), where a helical content of approximately 60% was observed. Penetratin has also been reported to adopt a *β*-sheet conformation under certain experimental conditions, e.g., during vesicle aggregation (*14*) and in experiments using deposited phospholipid bilayers (*24*). By contrast, for R_7W, TatP59W, and TatLysP59W, a random coil type of spectrum is obtained also when bound to DOPC/DOPG/DSPE-PEG (60/35/5) vesicles. The arginine-to-lysine substitution in TatLysP59W did not affect the peptide secondary structure, as the CD spectra of TatP59W and TatLysP59W are very similar. A random coil spectrum has previously been reported for Tat(47-57) (YGRKKRRQRRR) when bound to POPC/ POPG vesicles (*61*).

Peptide Translocation in LUVs. A key question for the understanding of the mechanism of uptake of cell-penetrating peptides is whether the peptides can enter cells via direct interaction with the membrane lipids. To determine whether CPPs are able to access the inner leaflet of large unilamellar vesicles, i.e., translocate across pure lipid bilayers, we have employed a method based on resonance energy transfer (RET). RET is the nonradiative transfer of excited-state energy from a donor to an acceptor, which results in quenching of the fluorescence of the donor. The efficiency of energy transfer, E, is often calculated according to

$$E = 1 - \frac{F_q}{F_0} \tag{5}$$

where F_0 and F_q is the unquenched and quenched donor fluorescence intensity, respectively (*41*). If the acceptor is fluorescent, energy transfer can also be detected as an increase in the fluorescence of the acceptor, according to (*41*)

$$E = \frac{OD_A(\lambda_D^{ex})}{OD_D(\lambda_D^{ex})}\left[\frac{F_{AD}(\lambda_A^{em})}{F_A(\lambda_A^{em})} - 1\right] \tag{6}$$

where $OD_A(\lambda^{ex}{}_D)$ and $OD_D(\lambda^{ex}{}_D)$ are the optical densities of the acceptor and the donor at the donor excitation wavelength, respectively. F_A and F_{AD} denote the fluorescence of the acceptor in the absence and in the presence of donor, respectively, at a wavelength suitable for the detection of acceptor emission ($\lambda^{em}{}_A$). Direct contribution from donor fluorescence at this wavelength must be corrected for (vide infra). For a donor−acceptor pair separated by a fixed distance, the transfer efficiency is related to the distance, *r*, according to

$$E_{pair} = \frac{R_0^{\,6}}{R_0^{\,6} + r^6} \tag{7}$$

where R_0 is the Förster distance, at which the efficiency of transfer is 50%.

Recently, Wimley and White presented an innovative implementation of quenching of tryptophan fluorescence by energy transfer (*33*), using a novel fluorescent lysolipid, lysoMC, which is a conjugate of methylcoumarin and lysophosphatidylethanolamine (lysoPE). Tryptophan and methylcoumarin constitute an excellent donor−acceptor pair with a good spectral overlap between emission from membrane-associated tryptophan residues and methylcoumarin absorbance, which has its maximum at ~335 nm (*33*). An R_0 value of approximately 25 Å has been estimated (*33*). The theoretical considerations of RET in membrane systems, where the donor and acceptor are not separated by a fixed distance, are not trivial (*62*). However, by careful examination of the concentration-dependence of tryptophan quench-

ing by lysoMC, it was shown that RET between tryptophan and lysoMC according to eq 5 is well described by eq 7 under the experimental conditions used. The use of a lysophospholipid as an anchor for the methylcoumarin moiety provides several advantages compared to fluorescently labeled diacyl phospholipids. Since lysophospholipids are water-soluble and can readily be exchanged between vesicles, preparation of asymmetrically labeled vesicles, i.e., vesicles with probe present exclusively in one of the leaflets of the lipid bilayer, is facilitated. For diacyl phospholipids to be asymmetrically incorporated into vesicles, methods based on rapid dilution of an organic solution of lipid into an aqueous solution containing vesicles are frequently employed. This can lead to an incomplete incorporation of the probe (*33*). Furthermore, since lysophospholipids are exchangeable between vesicles, the stability of the transbilayer asymmetry of the probe can be examined (*33*).

The method used to determine peptide topology in ref *33* is based on comparison of the quenching of tryptophan emission in two sets of liposomes: symmetrically labeled (lysoMC present in both leaflets) and asymmetrically labeled (lysoMC present in the outer leaflet only). Here, we have instead used an assay based on LUVs with lysoMC present in the inner leaflet only. By using a protocol involving transfer of lysoMC in the outer leaflet to acceptor particles, which are subsequently separated from the LUVs, vesicles with an almost complete asymmetry can be obtained (Persson et al., unpublished experiments). We accomplish this by mixing LUVs (100 nm diameter) symmetrically labeled with lysoMC (1 mol %) with large lipid particles, several microns in diameter (see Materials and Methods). The lipid particles are added in excess and serve as a reservoir for lysoMC, which equilibrates between the outer leaflets of the unilamellar vesicles and the lipid particles. After equilibration, the vesicles are separated from the particles by centrifugation and a small fraction of the vesicles is examined by fluorescence spectroscopy. The emission spectrum of methylcoumarin is bimodal under our experimental conditions, corresponding to the neutral form of the chromophore and its tautomer anion (*63*). The neutral methylcoumarin species has an emission maximum at approximately 400 nm, while the tautomer anion has an emission maximum at ~460 nm. The spectral properties of lysoMC can be utilized to assess the asymmetry of the probe in the vesicles after separation from the lipid particles, by selectively deprotonating lysoMC molecules in the outer leaflet. This is accomplished by exogenous addition of sodium hydroxide, thereby raising the pH in the surrounding solution to 11. The change in pH causes diminution of the emission peak at 400 nm for lysoMC present in the outer monolayer. The "washing" procedure involving equilibration with lipid particles and separation by centrifugation is repeated until a negligible amount of lysoMC remains in the outer leaflet of the vesicles, indicated by a lack of decrease in fluorescence intensity at 400 nm upon addition of sodium hydroxide. Under the experimental conditions used here, this is typically achieved after four or five cycles. A prerequisite for the use of asymmetrically labeled vesicles in RET measurements of peptide topology is, of course, that the lipid-anchored probe remains in the same leaflet during the time course of the experiment. This condition is met by lysoMC, the spontaneous flip-flop of which is slow ($t_{1/2} \sim$ days) (*33*). Throughout this study, asymmetrically labeled vesicles were prepared and used within 4 h.

Peptide translocation was studied by monitoring RET in samples with tryptophan-containing peptides added exogenously to inner leaflet-labeled vesicles. Since R_0 is about equal to the thickness of the hydrocarbon core of the lipid bilayer and both donor (tryptophan) and acceptor (lysoMC) are present at low concentrations in the membranes, transmembrane energy transfer should be weak, provided that the tryptophan does not penetrate deeply into the membrane. A small extent of RET is thus expected for compounds that do not cross the membrane. On the other hand, if the tryptophan-containing molecule is able to translocate across the membrane and reach the inner leaflet, an efficient energy transfer should be observed. As reference compounds, tryptophan octyl ester (TOE) and Ac-18A-NH_2 were used. TOE readily binds to and equilibrates across lipid bilayers (*33*). Ac-18A-NH_2 is largely α-helical when bound to lipid bilayers, with the helix axis oriented parallel with the bilayer plane, and does not translocate across the membrane (*33*, *64*−*67*). As mentioned earlier, energy transfer can be detected either as a decrease in the fluorescence intensity of the donor or as an increase in the fluorescence intensity of the acceptor molecule. When using inner leaflet-labeled vesicles to assay tryptophan topology, we find that measurements of the increase in acceptor fluorescence are more sensitive, and calculations according to eq 6 should thus be performed. However, since adsorption to surfaces is encountered for peptides (*15*) as well as for TOE (Persson et al., unpublished experiments), the exact concentration of donor in each sample is uncertain. In the analysis here, the RET efficiency is calculated simply as the percent increase in acceptor fluorescence. To allow a direct comparison between the efficiency of energy transfer in the samples, it is thus desirable that the ratio of donor and acceptor concentration is approximately equal in the samples, making the contribution from the first factor (OD_A/OD_D) on the right-hand side of eq 6 constant. Therefore, the peptide to lipid molar ratios were chosen so that the peptides would be essentially bound to the vesicles with an approximately equal concentration of membrane-associated tryptophan residues. The small deviations in donor concentration are not crucial for the experiment, since when multiple donors and acceptors are used, it is ultimately the acceptor concentration that determines the energy transfer efficiency (*41*). Thus, Ac-18A-NH_2, R_7W, TatP59W, and TatLysP59W, which contain one tryptophan, were added at a peptide to lipid molar ratio of 1:275, while penetratin, with two intrinsic tryptophan residues, was examined at a peptide to lipid molar ratio of 1:550. TOE was consequently added at a TOE:lipid ratio of 1:275. Figure 5 shows the bimodal emission spectrum of inner leaflet-labeled lysoMC vesicles in the absence (lower trace) and in the presence of TOE (upper trace) or Ac-18A-NH_2 (middle trace). Although an excitation wavelength of 260 nm was used in order to minimize direct excitation of lysoMC (*33*), the fluorescence intensity in the absence of donor is substantial. In the presence of a membrane-bound tryptophan-containing compound, the lysoMC fluorescence intensity increases, due to RET. For calculation of the extent of energy transfer, the increase in lysoMC fluorescence at 460 nm was used. Since the tryptophan emission spectrum overlaps in part with that of lysoMC and has a small, but

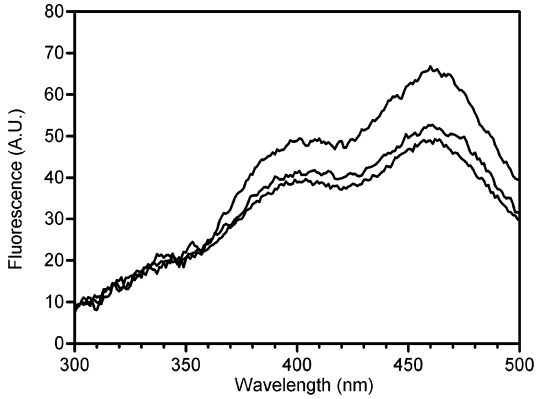

FIGURE 5: Detection of translocation across the membranes of large unilamellar vesicles (LUVs) by resonance energy transfer (RET) using tryptophan as donor and the fluorescent lysophospholipid lysoMC as acceptor. The figure shows the emission spectrum of LUVs containing lysoMC exclusively located in the inner leaflet, formed by removing lysoMC from the outer leaflet of symmetrically labeled vesicles (1 mol %). Spectra were recorded in the absence (lower trace) and in the presence of TOE (upper trace) or Ac-18A-NH_2 (middle trace). The tryptophan emission contribution to the spectrum has been subtracted, as described in the text. The addition of TOE results in a large increase in lysoMC fluorescence due to RET, indicating translocation across the membrane. Only a minor extent of RET is obtained upon addition of Ac-18A-NH_2, which remains in the outer leaflet of the vesicle membranes. Penetratin, R_7W, TatP59W, and TatLysP59W all yielded results similar to that of Ac-18A-NH_2, indicating that none of the peptides is able to translocate across the membranes of LUVs.

Table 5: Determination of Translocation of Peptides and TOE across the Membranes of Large Unilamellar Vesicles by Resonance Energy Transfer in Inner Leaflet-Labeled LysoMC Vesicles[a]

peptide	λ_{max} (nm)[b]	E (%)[c]
penetratin	336	5
R_7W	338	8
TatP59W	337	8
TatLysP59W	338	6
Ac-18A-NH_2	333	6
TOE[d]	333	38

[a] Polar extract of lipid soybean lecithin (see Materials and Methods). Peptide:lipid molar ratios were 1:275, except for penetratin (peptide:lipid ratio 1:500). [b] Tryptophan emission maximum using an excitation wavelength of 260 nm. [c] Calculated as $100\times(F_{AD}/F_A - 1)$ at 460 nm after correction for tryptophan emission. [d] Tryptophan octyl ester.

nonzero intensity at 460 nm, its contribution to the lysoMC spectrum must first be subtracted. This was accomplished by using the following procedure. First, the background spectrum of the lysoMC vesicles is subtracted from the spectrum measured after addition of the tryptophan-containing compound. In the resulting spectrum, the lysoMC contribution stems exclusively from RET. At wavelengths below 350 nm, however, only emission from tryptophan and vesicle background is observed. By comparing the signal at the wavelength of maximum tryptophan emission intensity (see Table 5) with the fluorescence intensity of the tryptophan-containing compound when bound to unlabeled vesicles at the same concentrations, the extent of quenching of the tryptophan moeity is obtained. The corresponding portion of the membrane-bound tryptophan emission spectrum in the absence of quencher can then be subtracted from the total emission spectrum in labeled vesicles, yielding a spectrum containing solely emission from the lysoMC vesicles, as in Figure 5. In the experiments presented in Figure 5, vesicles were formed from the same soybean lipid extract as in the giant vesicle study (vide infra). The emission obtained at wavelengths below 350 nm does not stem from lysoMC but from the soybean lipid extract and is not observed in vesicles formed from synthetic lipids. The calculated values of the extent of energy transfer for the compounds examined are summarized in Table 5. As expected, the addition of TOE to asymmetrically labeled vesicles was found to result in a large increase in lysoMC fluorescence intensity, approximately 38% at a TOE to lipid molar ratio of 1:275. The addition of the nontranslocating peptide Ac-18A-NH_2 to asymmetrically labeled vesicles yielded an increase in lysoMC fluorescence of approximately 6%. As shown in Table 5, penetratin, R_7W, TatP59W, and TatLysP59W all yielded values close to that of Ac-18A-NH_2, ranging from 5% to 8%, indicating that none of the peptides examined was able to translocate across the lipid membranes. The extent of energy transfer was also examined in asymmetrically labeled vesicles containing lysoMC exclusively in the outer leaflet, corresponding to 0.5 mol % of the total amount of lipids (data not shown). For all of the peptides, the extent of energy transfer was found to be much larger than in inner leaflet-labeled vesicles, with values ranging from 45 to 55%, further supporting the conclusion that the peptides are located in the outer leaflet.

There is, of course, a possibility that translocation of peptides across lipid bilayers requires specific lipid compositions in terms of charge density and lipid packing, especially considering the suggested translocation mechanism involving inverted micelles. To investigate the influence of lipid composition on the membrane topology, the lysoMC experiment was also performed using vesicles composed of DOPC/DOPG (60/40), EggPC/DOPG (60/40) and 100% DOPG. In all cases, similar results to those presented in Table 5 were obtained (data not shown).

Peptide Translocation in Giant Vesicles. The ability of peptides to translocate across vesicle membranes was also examined in giant vesicles. The vesicles were prepared by a dehydration/rehydration technique, known to produce both giant unilamellar vesicles (GUVs) and multilamellar vesicles (MLVs) (*54*, *55*). The unilamellar vesicles obtained by this method are typically 1−300 μm in diameter (*55*) and can thus readily be examined by microscopy. To determine the localization of peptides added to the solution, the peptides were labeled with carboxyfluorescein. In our previous study of the interaction of penetratin with giant unilamellar vesicles using fluorescence microscopy (*13*), we showed that the peptide was able to translocate across the vesicle membranes and reach the interior of the vesicles. In the present work, we compared the translocation ability of penetratin with that of R_7W, TatP59W, and TatLysP59W using confocal laser scanning microscopy, to see if there was any correlation between their ability to translocate across the membranes of giant vesicles and their cellular uptake efficiency.

The majority of the GUVs formed after addition of buffer (0.5 mL) were found to be associated with MLVs on the surface of the coverslip, but several GUVs that were not attached to MLVs were also obtained, both floating in the solution and sitting on the surface. The latter are denoted free-standing GUVs in the text. After equilibration for 15 min, a small volume of peptide stock solution (20 μL) was carefully added at the top of the droplet on the coverslip,

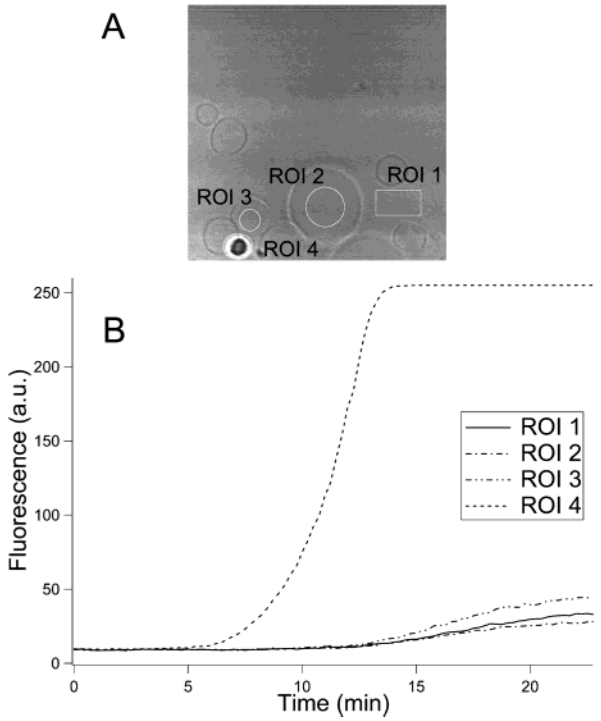

FIGURE 6: Detection of translocation of carboxyfluorescein-labeled peptides across the membranes of giant vesicles using confocal laser scanning microscopy. (A) Bright field image of an ensemble of giant vesicles on the coverslip surface. Several regions of interest (ROIs) are defined, in which the averaged fluorescence intensity (in arbitrary units on a scale ranging from 0 to 255) is measured. In the figure, ROI 1 is located in the surrounding buffer, ROI 2 is defined as the inside of a free-standing giant unilamellar vesicle (GUV), ROI 3 is defined as the inside of a GUV attached to a multilamellar vesicle (MLV), and ROI 4 is placed inside an MLV. (B) Time course of the fluorescence intensity in the ROIs in a focal plane located inside the interior of the vesicles. A small volume of peptide stock solution was carefully added at the top of the droplet on the coverslip, without perturbing the vesicles on the surface. With time, the measured fluorescence intensities increase as peptide diffuses to the vesicles in the observed region.

leaving the vesicles residing on the coverslip surface undisturbed. This allowed us to monitor the time course of peptide translocation as the added peptide molecules diffused into the focal plane (containing the vesicles) from the point of addition of peptide. An increase in fluorescence intensity was typically observed 10−15 min after peptide addition. Figure 6 shows the time course of the fluorescence intensity of a sample after the addition of TatLysP59W, to yield a final concentration of 4 μM. In the imaged liposomes (Figure 6A), several regions of interest (ROIs) are defined, and the plot (Figure 6B) shows the averaged fluorescence intensity in arbitrary units (on a scale ranging from 0 to 255) in the defined ROIs. In the experiment presented in Figure 6, ROI 1 is placed in the surrounding buffer, while ROI 2 is defined as the inside of a free-standing GUV and ROI 3 is located in the interior of a GUV attached to an MLV. ROI 4 is placed inside an MLV. At the start of the experiment, a low but nonzero background intensity is obtained. At about 6 min after initiation of the measurement, the fluorescence intensity starts to increase. This is most evident in the MLV (ROI 4), where a substantial amount of peptide binds to the many lipid bilayers. Interestingly, the fluorescence intensities in the surrounding buffer and inside the GUVs (ROI 1−3) increase simultaneously, suggesting that the peptide translocates rapidly across the vesicle membranes to the inside of the vesicles. The same phenomenon was observed for the other peptides investigated. After the time course measurement, several vesicles in the sample were imaged and the fluorescence intensities of the inside and the outside of the vesicles were compared. Figure 7A−D shows fluorescence images of free-standing GUVs in the presence of R_7W, TatP59W, TatLysP59W, and penetratin, respectively. In all cases, there is a strong peptide fluorescence emanating from the vesicle membranes. The intensity profile (Figure 7E) measured along the white line in Figure 7A shows that the R_7W fluorescence intensity in the interior of the vesicles is roughly equal to the intensity in the surrounding buffer, suggesting that the peptide has equilibrated across the vesicle membranes. Similar observations were made for all of the other peptides. Notably, TatLysP59W exhibited a somewhat stronger fluorescence intensity in the aqueous solution, suggesting a slightly weaker affinity for the membranes.

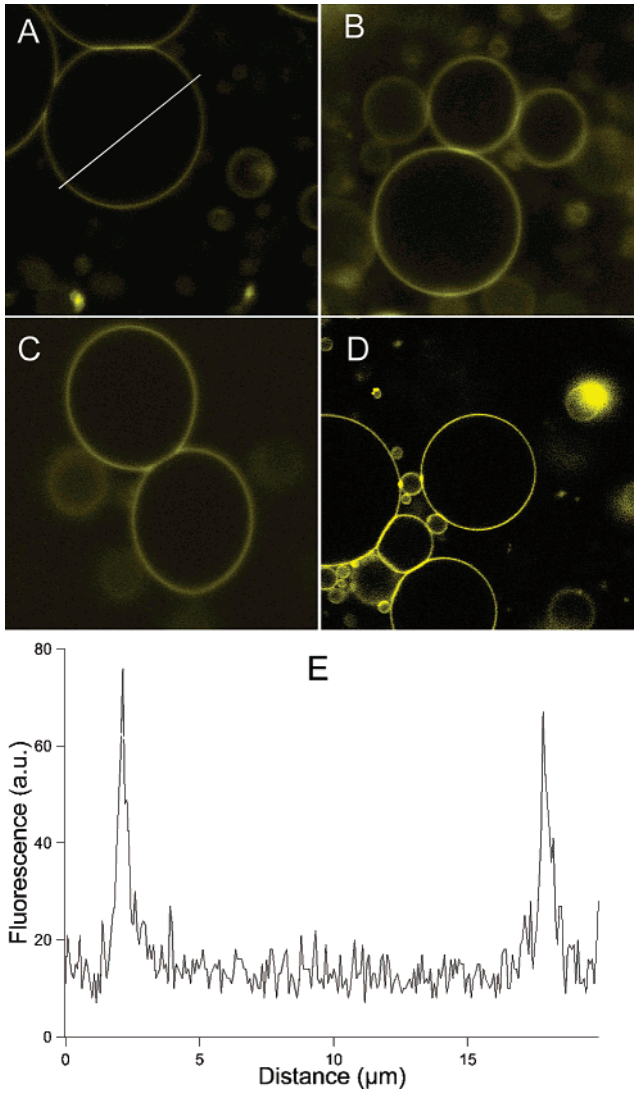

FIGURE 7: (A−E) Confocal laser scanning microscopy images of GUVs after addition of peptide and equilibration. Peptides were added to yield a final concentration of 4 μM. (A) R_7W, (B) TatP59W, (C) TatLysP59W, and (D) penetratin. (E) Fluorescence intensity profile corresponding to the white line indicated in (A).

Control experiments using photobleaching were performed to ensure that the fluorescence intensity observed in the interior of the vesicles was not due to out-of-focus fluores-

cence from membrane-associated peptide. When exciting a region inside the vesicles with the highest laser intensity for 30 s, rapid photobleaching was observed. With time, the fluorescence intensity in the interior of the vesicle was recovered, reaching the level observed prior to photobleaching within minutes (data not shown). The same phenomenon was observed for the fluorescence in the surrounding buffer. In another set of experiments, the focal plane was set to the level of the membrane facing the buffer (the "top" of the vesicle), and the fluorescence intensity in the membrane was measured. Then the focal plane was moved to the equatorial plane of the vesicle, and the sample was subjected to excitation with the highest laser intensity for 30 s. Immediately after photobleaching, the focal plane was returned to the membrane level and the fluorescence intensity was measured. No photobleaching of the peptide associated with the membrane was observed, showing that the fluorescence observed inside the vesicles was from peptide present in the aqueous interior of the vesicles.

The integrity of the vesicle membranes was examined using a fluorescently labeled 20-mer oligonucleotide. After addition of oligonucleotide (1 μM final concentration), the fluorescence inside the vesicles and in the buffer was examined. The strongly anionic oligonucleotide did not bind to the negatively charged vesicle membranes and, consequently, a strong and uniform fluorescence was obtained in the aqueous solution. As to the vesicles, large variations between different kinds of vesicles were observed: MLVs were apparently more or less completely permeable to the oligonucleotide, as a strong fluorescence was observed throughout the inside of MLVs. In some cases, the fluorescence intensity was even higher than in the surrounding buffer. Likewise, GUVs associated with MLVs exhibited strong fluorescence, showing that no intact barrier exists. Free-standing GUVs, on the other hand, were generally less permeable to oligonucleotide, since the fluorescence inside was clearly weaker than in the surrounding aqueous solution (Figure 8A), as illustrated by the line profile (Figure 8B).

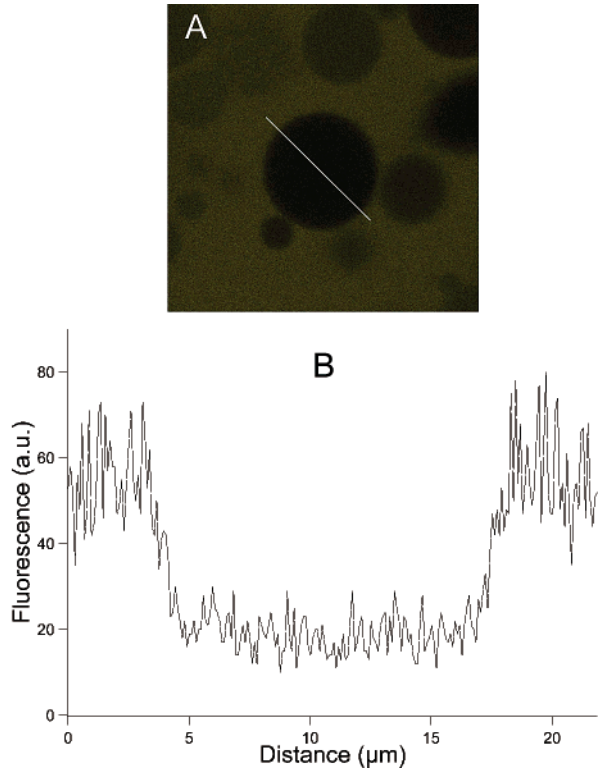

FIGURE 8: (A) Confocal laser scanning microscopy image of GUVs after addition of a fluorescein-labeled 20-mer oligonucleotide. (B) Fluorescence intensity profile corresponding to the white line indicated in panel A.

DISCUSSION

Membrane Binding. The binding of the peptides penetratin, TatP59W, TatLysP59W, and R_7W to vesicle membranes has been examined. By using vesicles with 5% of PEG-lipid conjugates, vesicle aggregation induced by the peptides can be avoided (Thorén et al., unpublished experiments), which would otherwise prevent proper spectroscopic measurements of the binding. The inclusion of hydrophilic PEG chains is assumed to have no significant effect on the overall affinity of the peptides for the liposomal membranes, as the binding data for penetratin obtained here agree quite well with our previous study on penetratin and vesicles without the PEG-lipid conjugate (*15*). The binding isotherms presented differ though, due to differences in the calculation of the membrane-bound peptide to lipid molar ratio, *r*. In our previous study, we assumed access of penetratin to both the inner and the outer leaflets of the vesicle membrane, while only the outer leaflet is considered accessible in this work, in light of the LUV translocation study. Also, differences in the determination of peptide concentration somewhat influence the calculations, see Materials and Methods. The binding parameters for penetratin agree well with those obtained for the binding of penetratin to DOPC/DOPG/ DSPE-PEG (60/37.5/2.5) (Persson et al., unpublished experiments).

The binding of basic, hydrophilic peptides to membranes containing acidic lipids involves a complex interplay between electrostatic attraction, hydrophobic interactions and dehydration effects. Penetratin, TatP59W, TatLysP59W, and R_7W were all found to associate strongly with vesicles composed of DOPC/DOPG/ DSPE-PEG (60/35/5), i.e., containing 40% negatively charged lipid. To compare the extent of binding of the different peptides, we analyzed the binding isotherms according to a binding model separating electrostatic and hydrophobic contributions (*32*). Although simplistic, this model, based on the Gouy−Chapman theory, has been successfully applied to describe the membrane association of a number of peptides (*32*, *61*, *68*−*71*).

The surface charge density, σ, of membranes composed of zwitterionic and anionic lipids is given by

$$\sigma = (e_0/A_L)\frac{-X_{AL}(1 - X_{Na}) + z_p r}{1 + (A_P/A_L)r} \qquad (8)$$

where e_0 is the elementary charge, A_L the area per lipid molecule, A_P the effective area of the peptide in the membrane, z_p the effective charge of the peptide, and X_{AL} the mole fraction of anionic lipid in the membrane. A_L was assumed to be equal for DOPC, DOPG, and DSPE-PEG and was set to 70 Å^2. The actual value of A_P is not known for the peptides investigated here. However, since *r* never exceeds 0.055 in our experiments, the contribution from the correction term for peptide insertion, $(A_P/A_L)r$, is small compared to unity. The choice of A_P is thus not critical for the calculations. We have used an A_P of 100 Å^2, which is

Table 6: Summary of Parameters for Peptide Binding to Vesicles of DOPC/DOPG/ DSPE-PEG (60/35/5)

peptide	K_p (M^{-1})[a]	z_p[b]
penetratin	836	5.7
R_7W	307	5.1
TatP59W	34	5.0
TatLysP59W	5	4.5

[a] Surface partition constant. [b] Effective peptide charge.

the estimated insertion area of Tat(47−57) in lipid monolayers of POPC and POPG (*61*). The reduction of the surface charge density due to counterion binding is accounted for by including X_{Na}, which denotes the mole fraction of anionic lipid associated with Na^+. X_{Na} is calculated by assuming a Langmuir adsorption isotherm

$$X_{Na} = \frac{K_{Na}C_{M,Na}}{1 + K_{Na}C_{M,Na}} \quad (9)$$

where K_{Na} is the Na^+ binding constant, taken as 0.6 M^{-1} for DOPG (*72*) and assumed to be equal for DSPE-PEG. $C_{M,Na}$ is the concentration of sodium ions in the close proximity of the membrane surface. $C_{M,Na}$ is connected to the bulk equilibrium concentration, $C_{eq,Na}$, and the surface potential, ψ_0, via a Boltzmann distribution

$$C_{M,Na} = C_{eq,Na}\exp(-\psi_0 F/RT) \quad (10)$$

where F is the Faraday constant, R the gas constant, and T the absolute temperature.

The surface potential can be determined by combining eq 8 with the Gouy−Chapman equation

$$\sigma^2 = 2000\epsilon_0\epsilon_r RT\sum_i C_{i,eq}(e^{-z_i F\psi_0/RT} - 1) \quad (11)$$

where ϵ_0 is the permittivity in a vacuum, ϵ_r denotes the relative dielectric permittivity of water, $C_{i,eq}$ is the bulk concentration of the ith electrolyte, and z_i is its signed valency. The peptide concentration immediately above the membrane surface, C_M, can be calculated according to

$$C_M = C_f\exp(-z_p F\psi_0/RT) \quad (12)$$

which accounts for the electrostatic attraction between the peptide and the membrane. The membrane binding can now be described by a surface partition equilibrium

$$r = K_p C_M \quad (13)$$

where K_p is the surface partition constant.

Since both the effective peptide charge, z_p, and the surface potential are unknown, the above set of equations must be solved by iteration. By assuming a value for z_p, eqs 8−12 were solved for each pair of r and C_f values, and the resulting C_M values were plotted against r. This procedure was repeated for a range of z_p values in search of the z_p that corresponds to the best fit to the experimental data according to eq 13. Table 6 shows the optimal values of z_p and K_p for the peptides under investigation and the corresponding theoretical binding isotherms are shown as solid lines in Figure 1. Although it is possible that the inclusion of DSPE-PEG slightly influences the peptide binding by some mechanism not included in the binding model (Persson et al., unpublished experiments), the fit to the experimental data is quite good. For all four peptides, the calculated z_p value is smaller than the formal charge. This effect is attributed to discrete charge effects (*73*, *74*), separation of charges in the peptide (*75*, *76*) and effects of associated counterions (*73*). Notably, the Tat peptides, which have a formal charge of +8, were found to have a smaller effective charge than penetratin and R_7W, which carry seven positive charges. The K_p values are moderate, reflecting a weak hydrophobic interaction between the peptides and the vesicle membranes. K_p for penetratin differs from the binding constant (80 M^{-1}) we reported earlier (*15*). As mentioned above, this is mainly due to the fact that we in this study have established that penetratin remains in the outer leaflet of LUVs, while the peptide was earlier assumed to have access to the inner leaflet of the vesicles, based on a study using giant vesicles (*13*). For TatP59W, the measured K_p is slightly higher than the value reported for Tat(47−57) (*61*). The differences can be ascribed to the amidation of the C-terminus in TatP59W, which increases the overall hydrophobicity of the peptide, but also to the slightly different amino acid sequences of the two peptides. The peptide binding can be further characterized in terms of the total free energy of binding according to

$$\Delta G = -RT\left[\ln 55.5 + \ln K_p + \ln\left(\frac{C_M}{C_f}\right)\right] \quad (14)$$

where ln 55.5 provides the cratic contribution (*77*), which amounts to −2.4 kcal/ mol, ln K_p provides the hydrophobic contribution to the binding energy and $\ln(C_M/C_f) = -z_p F\psi_0/RT$ provides the electrostatic contribution, evaluated at infinite low degree of binding where the surface potential ψ_0 has the value it would have in the complete absence of charged peptide. The calculated value for the electrostatic free energy contribution is thus directly related to the effective peptide charge z_p and is very similar for R_7W (−7.2 kcal/mol) and TatP59W (−7.1 kcal/mol), slightly higher for penetratin (−8.1 kcal/mol) and somewhat lower for TatLysP59W (−6.4 kcal/ mol).

For penetratin, the experimentally determined hydrophobic contribution to the binding energy amounts to −4.0 kcal/ mol. This hydrophobic energy contribution can be viewed as a combination of partitioning of the peptide from the aqueous phase into the membrane and the formation of inter- or intramolecular hydrogen bonds as the peptide forms a secondary structure. Assuming that the two tryptophan residues of penetratin penetrate to a similar extent into the membrane, the data from the study of quenching by brominated lipids indicate a tryptophan position approximately 10 Å from the bilayer center. From this observation alone, however, we cannot determine the position of the peptide as a whole within the interfacial region, nor to what extent the peptide penetrates into the hydrocarbon region of the membrane. For penetratin, a significant favorable energy contribution is obtained from the formation of an α-helical structure. Our previous study of penetratin binding to DOPC/DOPG vesicles indicated a helical content of ∼60%, regardless of DOPC/DOPG ratio (*15*), at low peptide to lipid molar ratios where no vesicle aggregation occurs. A similar CD spectrum was obtained in vesicles containing 5 mol % DSPE-

PEG in the present study (Figure 4). The formation of an α-helix can compensate for the increase in free energy associated with partitioning of the relatively hydrophilic peptide into the membrane. The charged arginine and lysine residues especially give unfavorable contributions to the partitioning of the peptide into the membrane interface (*78*).

The experimental values for the hydrophobic free energy of binding for R_7W, TatP59W, and TatLysP59W in our study are −3.4, −2.1, and −1.0 kcal/mol, respectively. The CD data indicate that none of the three peptides forms an ordered structure upon association with the vesicle membranes. Partitioning of the entire peptides, which are rich in arginine and lysine residues, into the bilayer thus seems unlikely. It has been suggested that highly charged hydrophilic peptides without a significant fraction of hydrophobic residues, e.g., oligolysines (*79*, *80*), do not penetrate the interface of lipid membranes but assume a position several Ångströms above the lipid headgroups. This is attributed to a dehydration effect that would occur when the charged peptide approaches the membrane interface (*80*−*83*). Nevertheless, in the case of R_7W, TatP59W, and TatLysP59W, the blue shift and increase in quantum yield observed for the tryptophan residues of these peptides is indicative of transfer from the aqueous phase to the less polar environment of the lipid bilayer. Furthermore, our measurements of the quenching of tryptophan fluorescence by acrylamide and by brominated lipids (Tables 2 and 4) suggest that the tryptophans of R_7W, TatP59W, and TatLysP59W all penetrate into the vesicle bilayers, ∼10 Å from the bilayer center, as for penetratin. One could speculate that the C-terminal part of these peptides, containing the hydrophobic tryptophan residue and the amidated C-terminus, dips down into the membrane interior, while the highly charged N-terminal part is localized somewhere in the membrane interface. This would result in less unfavorable energy contributions than transfer of the entire peptide into the membrane interface. In this context, it is worth mentioning that for class A amphipathic helixes, a "snorkel" model has been proposed, to explain the observation of penetration of the helix into the hydrophobic interior of lipid bilayers despite a high content of positively charged amino acid residues (*64*, *84*). In this model, extension of the hydrocarbon chains of arginine and lysine residues toward the headgroup region of the bilayer permits their charged moieties to be located in a polar environment although the helix axis resides in the hydrocarbon region of the lipid bilayer. Such an arrangement would aid the penetration of the C-terminal part of R_7W, TatP59W, and TatLysP59W into the lipid bilayers.

The lysine-substituted Tat peptide has a weaker membrane affinity than its parent peptide, mainly due to the weaker hydrophobic contribution. Differences in membrane affinity between oligoarginines and oligolysines have been reported earlier (*79*, *85*). Indeed, computer simulations have suggested that there exists a strong and specific interaction between arginine residues and the phosphate group of membrane lipids (*86*).

Quenching Experiments. The presence of intrinsic tryptophan residues in the peptides allows comparison of the peptides by fluorescence quenching experiments. As reference compounds, a well characterized 18-residue amphipathic class A peptide (Ac-18A-NH_2) and tryptophan octyl ester (TOE) were used. First, the neutral, water-soluble quencher acrylamide was used (Table 2). The measured Stern−Volmer quenching constants (K_{SV}) for Ac-18A-NH_2 agree well with published data (*64*). The quenching constants for Ac-18A-NH_2, penetratin, R_7W, TatP59W, and TatLysP59W in buffer were found to be 60−90% of that of free tryptophan. The K_{SV} values are comparable to K_{SV} values obtained for other moderately hydrophobic peptides, e.g., melittin (12.5 M^{-1}) (*87*) and nisin (*71*). Together with the finding that the peptides exhibit an emission maximum close to that of free tryptophan, this shows that the tryptophan residues are readily accessible to the solvent, indicating that the peptides are not aggregated when dissolved in buffer. Addition of DOPC/DOPG (60/40) vesicles, on the other hand, is accompanied by a blue shift in tryptophan fluorescence and an increase in intensity. The tryptophan residue is protected from quenching by acrylamide, as evidenced by a strong decrease in K_{SV}, indicating that the tryptophan is inserted into the lipid bilayer. For acrylamide concentrations >0.1 M, the Stern−Volmer plots exhibit an upward curvature (data not shown), indicating the presence of static quenching (*41*). The deviation from linearity is, however, smaller for membrane-bound peptides, indicating that the static quenching is prevented by peptide insertion into the bilayer. When calculating the normalized accessibility factor (naf) for the various peptides, very similar results are obviously obtained (Table 2), which would suggest a similar extent of shielding from acrylamide quenching. However, the reduction of the quenching constants upon peptide binding cannot be taken as a direct measure of the relative accessibility of the tryptophan residues to the solvent. Other factors may also influence the results, such as the slower translational diffusion of the peptide when it is associated with the vesicle membrane and changes in tryptophan fluorescence lifetimes upon membrane binding (*65*). Assuming that these factors contribute approximately equally to the reduction of the acrylamide quenching constants for the peptides investigated, the data suggest that the tryptophan residues of the various peptides are inserted into the bilayer to a similar extent. The smaller naf value for penetratin could reflect its stronger membrane affinity, leading to a smaller population of free peptide. Without detailed fluorescence lifetimes data for the peptides, however, a quantitative analysis of the quenching process is not possible. The K_{SV} values obtained for penetratin in buffer and the presence of DOPC/DOPG vesicles are close to the quenching constants reported earlier for penetratin in Tris buffer and associated with EggPC/phosphatidylserine LUVs (*22*), but differ from those reported in another study of penetratin association with POPG/ POPC small unilamellar vesicles (*18*).

The studies of the quenching of tryptophan fluorescence by brominated lipids yield more information and are in agreement with the acrylamide quenching data for all peptides investigated. A tryptophan insertion depth of 10−11 Å from the bilayer center was obtained, according to both DA and PM analysis. The tryptophan moiety of TOE is seemingly inserted somewhat deeper, on an average residing 9.6 Å from the bilayer center according to distribution analysis and 10.2 Å according to PM. This is deeper than what has been reported previously by Ladokhin et al., using vesicles composed entirely of brominated lipids (10.3−11.3 Å) (*60*) and Abrams, using spin-labeled phospholipids incorporated into DOPC vesicles (13.5 Å) (*47*). At this point we cannot explain this discrepancy, but note that the

membranes used in this study are anionic whereas those used in previous studies have been zwitterionic. As a control of the accuracy of our measurements, melittin was investigated. The tryptophan penetration depth of melittin is in excellent agreement with results from a study on vesicles very similar to ours containing 60% anionic DOPG (*58*) as well as with other results (*48*, *49*, *59*, *60*). Yau et al. have shown that four tryptophan analogues, including the tryptophan chromophore indole, as well as a tryptophan-containing tripeptide show a strong preference for the membrane interfacial region residing close to the glycerol groups (*88*). The authors hypothesize that there might exist a balance between the hydrophobic effect pushing the tryptophan residue toward the hydrocarbon region and electrostatic interactions making the hydrated headgroup region favorable. It has been established that aromatic residues, particularly tryptophan and tyrosine, in integral membrane proteins are often found at the lipid/water interface (*89*−*91*). The aromatic residues have been suggested to function as "floats" that position transmembrane helices within the bilayer (*92*). Nevertheless, there are numerous reports on amphipathic peptides that insert their tryptophan residues into the hydrocarbon core region of the membrane. These peptides predominantly bind with an orientation parallel to the membrane surface (*58*, *59*, *93*−*97*).

Peptide Translocation in Large Unilamellar Vesicles. We recently showed that penetratin, as well as some of analogues of penetratin, does not translocate across the membranes of large, unilamellar vesicles of various lipid compositions (Persson et al., unpublished experiments). In the present study, the lysoMC assay for translocation of tryptophan-containing compounds (Table 5) clearly indicates that none of the peptides penetratin, R_7W, TatP59W, and TatLysP59W is able to translocate across the membranes of large unilamellar vesicles under the experimental conditions used here. This is shown by the minor extent of resonance energy transfer between the tryptophan residues of the exogenously added peptides and lysoMC, present in the inner leaflet of the vesicle membranes. A similar, low efficiency of energy transfer was obtained for Ac-18A-NH_2, which has been shown not to translocate across the membranes of POPC and POPG LUVs (*33*). This is likely to be the case also in the present study. The observation of a nonzero efficiency of energy transfer (∼5−10%) for all the peptides may have two explanations. First, there is a possibility that the distribution of lysoMC lipids in the vesicle membranes is not perfectly asymmetric, i.e., that some lysoMC molecules remain in the outer leaflet. However, the sensitive fluorescence assay for lysoMC asymmetry shows that the remaining lysoMC in the outer leaflet after five "washing" cycles amounts to only ∼1% of the amount of the lysoMC present in the outer leaflet of the symmetrically labeled vesicles. This very small fraction of lysoMC could not have any significant impact on the results. The lysoMC asymmetry might be lost in the presence of membrane-bound peptides, due to peptide-induced transbilayer movement of lipids, flip-flop. This possibility can, however, be ruled out from experiments involving exchange of lysoMC between symmetrically labeled vesicles and vesicles containing the nonexchangeable lipid probe NBD-PE, which acts as a quencher of lysoMC fluorescence. Thus, for TOE and Ac-18A-NH_2, it has been established that no flip-flop be induced in POPC or POPG vesicles (*33*). The same experiments applied to our vesicles confirmed that neither TOE, Ac-18A-NH_2 nor penetratin induced flip-flop (data not shown). Given the very similar RET results (Table 5), this is concluded to be the case also for the other peptides.

The second, and most probable explanation for the observed RET for the peptides examined, is instead transmembrane energy transfer. The lysoMC method relies on the assumption that the tryptophan residues in the compounds investigated reside near the membrane interface rather than deep in the hydrocarbon core of the membrane. A shallow bilayer penetration of tryptophan yields a small transmembrane energy transfer to lysoMC molecules located in the opposite leaflet of the membrane. Tryptophans located at the bilayer center, on the other hand, would be equally quenched by lysoMC present in either leaflet. To be able to accurately interpret the quenching data, it is therefore desirable to establish the penetration depth of the tryptophan residues in the compounds investigated. Deeply buried tryptophans generally have an emission maximum below 320 nm, while interfacial tryptophans exhibit emission maxima at wavelengths between 321 and 339 nm (*33*, *98*). All the compounds examined here, including TOE, fall into to the latter category. The emission maximum wavelength may not, however, be taken as a direct measure of the depth of penetration for the tryptophan residue, since the position of the emission maximum is the result of a combination of shielding of tryptophan from the aqueous solution by insertion into the membrane and effects due to peptide-induced alterations of the water penetration into the membrane. However, the data from the study of quenching of tryptophan fluorescence by brominated lipid, discussed above, unequivocally showed that the tryptophans of all the compounds examined here reside approximately in the same region of the lipid bilayer. This justifies the direct comparison of the RET efficiency for the peptides examined. Although the penetration depth was only determined for a lipid composition of PC/PG (60/40), a similar membrane penetration for the peptides in this study is likely for the other vesicle compositions examined in the lysoMC study. This strongly supports the conclusions of the translocation study, that all of the peptides bind to the vesicle membranes and remain in the outer leaflet.

Peptide translocation in LUVs was studied at low peptide to lipid molar ratios, where essentially all of the peptide is bound to the lipid membranes. The binding is instantaneous, as indicated by the immediate appearance of blue shift and increase in intensity of the tryptophan emission spectrum upon association of the peptide with unlabeled vesicles. No change in tryptophan fluorescence is thereafter observed with time. Likewise, the lysoMC assay yielded the same results regardless of the elapsed time between peptide addition and the beginning of data acquisition, which was varied between 10 s and 30 min (data not shown). This shows that no slow translocation process takes place. Such translocation has been reported for pore-forming peptides, e.g., magainin and melittin (*99*, *100*). In the case of penetratin, it has earlier been shown that no slow peptide translocation due to pore formation occurs (*20*). Our results are supported by recent binding studies of Tat(47−57), which suggest binding of the peptide to the vesicle outside only (*61*).

Peptide Translocation in Giant Unilamellar Vesicles. In a previous study, we showed by fluorescence microscopy

that penetratin is able to translocate across the membranes of giant unilamellar vesicles (GUVs) (*13*). Since the results of the lysoMC assay showed that this is not the case for large unilamellar vesicles (LUVs), the interaction of CPPs with giant vesicles was reexamined, using confocal laser scanning microscopy, to establish whether the observed differences in translocation ability was due to the choice of lipid model system. Contrary to the LUV experiments, R_7W, TatP59W, and TatLysP59W, and penetratin were found to be able to translocate across the membranes of GUVs and reach the interior of the vesicles (Figure 7). By adding the peptide at the top of the droplet on the coverslip and allowing the peptide to diffuse to the vesicles on the surface, rather than mixing the solution, it was possible to monitor the time-course of peptide internalization (Figure 6). The results show that the translocation process is rapid, resulting in a fast equilibration across the GUV membranes for all the peptides examined.

The control experiments using a 20-mer oligonucleotide labeled with fluorescein show that the giant vesicles obtained by the dehydration/rehydration method used are very heterogeneous as to their barrier properties. The MLVs are obviously not composed of closed bilayer structures, as the passive diffusion of the negatively charged oligonucleotide into the interior of the MLVs is not hindered. GUVs that were attached to the MLVs were also permeable to the oligonucleotide. One could speculate that the oligonucleotide could access the interior of these GUVs via the MLVs that they were connected to, since the nature of the vesicle junction is unknown. Free-standing GUVs (vesicles not attached to an MLV), on the other hand, were generally less permeable to the oligonucleotide (Figure 8), suggesting that the bilayers of these GUVs were intact and nonleaky. Notably, the access of the peptides to the interior of such free-standing GUVs was not restricted.

To sum up the translocation experiments, important differences were observed between the two model systems, although the same lipid composition was used. While none of the peptides was able to translocate across the membranes of LUVs, all of them readily equilibrated across GUV membranes. For the peptides examined in this study, it is thus obvious that the choice of model system determines the ability of the peptides to traverse the lipid bilayers. This explains the contradicting results reported regarding the translocation ability of penetratin (*13*, *20*). We do not know the reason for the observed differences in barrier properties of the LUV and GUV membranes, but note that similar observations have been reported for proteins (DNases and RNases) added either to GUVs formed by electroformation or LUVs prepared by extrusion (*101*). The differences were attributed to the fluid and dynamic behavior of GUVs, compared to the relatively compact structure of LUVs (*101*). However, the current lack of knowledge of the precise structural details of GUVs makes it difficult to determine whether the differences in the translocation of CPPs in LUVs and GUVs reported here are due to the nature of the peptide-lipid interactions or to the intrinsic properties of the two model systems. One important issue, which must be investigated in future studies, is which of the two model systems that represents the better model for biological membranes.

CONCLUSION

In this paper, the membrane binding and translocation of four different peptides were examined, to determine whether differences in their interactions with lipid model membranes could explain their vastly different uptake characteristics in live cells (*27*). The affinity of TatLysP59W for the surfaces of cells is very weak compared to penetratin, TatP59W, and R_7W. Although a slightly weaker binding to phospholipid vesicles was observed for TatLysP59W, compared to that for the other peptides, the relatively small difference in lipid affinity cannot explain the very large difference in cell association observed in live cells. It is thus more likely, that variations in affinity for other constituents on the cell surface, such as glycosaminoglycans, are responsible for the observed differences in cell surface binding. For Tat(47−57), a strong affinity for heparan sulfate has been reported (*61*), and binding to heparan sulfate has also been reported to be essential for translocation of the Tat protein (*102*, *103*).

The issue of whether the peptides are able to translocate across protein-free lipid bilayers was also addressed, in view of results from cell studies indicating R_7W to be internalized by cells by an energy-independent mechanism, while penetratin was taken up by endocytosis and TatLysP59W was not taken up at all (*27*). Two different model systems were used: large unilamellar vesicles and giant unilamellar vesicles. Surprisingly, in the former model system, none of the peptides was able to translocate across the lipid bilayers, while in the latter, all of the peptides could traverse the membranes. There is thus no simple correlation between the results for peptide translocation in model systems and cellular uptake, and we conclude that under the present conditions, peptide−lipid interactions alone cannot explain the mechanism of cellular uptake of CPPs.

ACKNOWLEDGMENT

We thank Michal Tokarz for help with the preparation of giant vesicles and Christina Brattwall, Petter Isakson and Åsa Nilsson for help with the peptide synthesis. Professor Kristina Luthman is acknowledged for giving us access to the peptide synthesizer. Anders Karlsson, Roger Karlsson, Max Davidson, and Jon Sinclair are acknowledged for interesting discussions on the preparation and properties of giant vesicles. Karin Oscarsson and Åsa Nilsson are acknowledged for technical assistance. Dr Bo Albinsson and Mattias Larsson are acknowledged for help with FTIR measurements. The confocal microscopy study was conducted at the Centre for Biophysical Imaging at Chalmers, which is financed by SWEGENE.

APPENDIX

For calculation of the binding isotherms, a procedure involving least-squares projection in combination with singular value decomposition (SVD) was used (*15*, *104*). The spectra were collected as columns with one intensity value per wavelength in a matrix of data *D*. This matrix was factorized by SVD according to

$$D = USV^T \tag{A1}$$

where *U* and *V* have orthonormal columns ($U^TU = V^TV = I$) and *S* is zero except along the diagonal which contains

the nonnegative singular values. It was found that only two singular values were significantly larger than zero and that they were the only singular values associated with nonrandom *U* columns. This is consistent with the hypothesis that two species, free and bound peptide, within experimental errors, account for the emission spectra of the whole titration:

$$D \approx RC^T \tag{A2}$$

where *R* is the reference spectra matrix and *C* is the peptide concentration matrix. *R* thus has two columns, the emission spectra of free and bound peptide at unit concentration, respectively, and the two columns of *C* contain the concentrations of free and membrane-bound peptide, C_f and C_b, in the titration. The concentrations *C* could be obtained by a least-squares projection of the emission spectra in *D* on the space of *R*:

$$C^T = (R^T R)^{-1} R^T D \tag{A3}$$

To ensure a negligible concentration of free peptide when measuring the reference spectrum of bound peptide, an excess lipid concentration was used.

REFERENCES

1. Schwarze, S. R., and Dowdy, S. F. (2000) In vivo protein transduction: intracellular delivery of biologically active proteins, compounds and DNA, *Trends Pharmacol. Sci. 21*, 45−48.
2. Schwarze, S. R., Hruska, K. A., and Dowdy, S. F. (2000) Protein transduction: unrestricted delivery into all cells? *Trends Cell Biol. 10*, 290−295.
3. Lindgren, M., Hällbrink, M., Prochiantz, A., and Langel, Ü. (2000) Cell-penetrating peptides, *Trends Pharmacol. Sci. 21*, 99−103.
4. Wadia, J. S., and Dowdy, S. F. (2002) Protein transduction technology, *Curr. Opin. Biotechnol. 13*, 52−56.
5. Derossi, D., Joliot, A. H., Chassaing, G., and Prochiantz, A. (1994) The third helix of the Antennapedia homeodomain translocates through biological membranes, *J. Biol. Chem. 269*, 10444−10450.
6. Derossi, D., Calvet, S., Trembleau, A., Brunissen, A., Chassaing, G., and Prochiantz, A. (1996) Cell internalization of the third helix of the Antennapedia homeodomain is receptor-independent, *J. Biol. Chem. 271*, 18188−18193.
7. Vivès, E., Brodin, P., and Lebleu, B. (1997) A truncated HIV-1 Tat protein basic domain rapidly translocates through the plasma membrane and accumulates in the cell nucleus, *J. Biol. Chem. 272*, 16010−16017.
8. Vivès, E., Granier, C., Prevot, P., and Lebleu, B. (1997) Structure−activity relationship study of the plasma membrane translocating potential of a short peptide from HIV-1 Tat protein, *Lett. Pept. Sci. 4*, 429−436.
9. Mitchell, D. J., Kim, D. T., Steinman, L., Fathman, C. G., and Rothbard, J. B. (2000) Polyarginine enters cells more efficiently than other polycationic homopolymers, *J. Pept. Res. 56*, 318−325.
10. Futaki, S., Suzuki, T., Ohashi, W., Yagami, T., Tanaka, S., Ueda, K., and Sugiura, Y. (2001) Arginine-rich peptides. An abundant source of membrane-permeable peptides having potential as carriers for intracellular protein delivery, *J. Biol. Chem. 276*, 5836−5840.
11. Suzuki, T., Futaki, S., Niwa, M., Tanaka, S., Ueda, K., and Sugiura, Y. (2002) Possible existence of common internalization mechanisms among arginine- rich peptides, *J. Biol. Chem. 277*, 2437−2443.
12. Berlose, J. P., Convert, O., Derossi, D., Brunissen, A., and Chassaing, G. (1996) Conformational and associative behaviours of the third helix of antennapedia homeodomain in membrane-mimetic environments, *Eur. J. Biochem. 242*, 372−386.
13. Thorén, P. E. G., Persson, D., Karlsson, M., and Nordén, B. (2000) The Antennapedia peptide penetratin translocates across lipid bilayers − the first direct observation, *FEBS Lett. 482*, 265−268.
14. Persson, D., Thorén, P. E. G., and Nordén, B. (2001) Penetratin-induced aggregation and subsequent dissociation of negatively charged phospholipid vesicles, *FEBS Lett. 505*, 307−312.
15. Persson, D., Thorén, P. E. G., Herner, M., Lincoln, P., and Nordén, B. (2003) Application of a novel analysis to measure the binding of the membrane- translocating peptide penetratin to negatively charged liposomes, *Biochemistry 42*, 421−429.
16. Magzoub, M., Kirk, K., Eriksson, L. E. G., Langel, U., and Gräslund, A. (2001) Interaction and structure induction of cell-penetrating peptides in the presence of phospholipid vesicles, *Biochim. Biophys. Acta-Biomembr. 1512*, 77−89.
17. Magzoub, M., Eriksson, L. E. G., and Gräslund, A. (2002) Conformational states of the cell-penetrating peptide penetratin when interacting with phospholipid vesicles: effects of surface charge and peptide concentration, *Biochim. Biophys. Acta-Biomembr. 1563*, 53−63.
18. Magzoub, M., Eriksson, L. E. G., and Gräslund, A. (2003) Comparison of the interaction, positioning, structure induction and membrane perturbation of cell-penetrating peptides and non-translocating variants with phospholipid vesicles, *Biophys. Chem. 103*, 271−288.
19. Lindberg, M., and Gräslund, A. (2001) The position of the cell penetrating peptide penetratin in SDS micelles determined by NMR, *FEBS Lett. 497*, 39−44.
20. Drin, G., Demene, H., Temsamani, J., and Brasseur, R. (2001) Translocation of the pAntp peptide and its amphipathic analogue AP-2AL, *Biochemistry 40*, 1824−1834.
21. Drin, G., Mazel, M., Clair, P., Mathieu, D., Kaczorek, M., and Temsamani, J. (2001) Physico-chemical requirements for cellular uptake of pAntp peptide − Role of lipid-binding affinity, *Eur. J. Biochem. 268*, 1304−1314.
22. Christiaens, B., Symoens, S., Vanderheyden, S., Engelborghs, Y., Joliot, A., Prochiantz, A., Vandekerckhove, J., Rosseneu, M., and Vanloo, B. (2002) Tryptophan fluorescence study of the interaction of penetratin peptides with model membranes, *Eur. J. Biochem. 269*, 2918−2926.
23. Bellet-Amalric, E., Blaudez, D., Desbat, B., Graner, F., Gauthier, F., and Renault, A. (2000) Interaction of the third helix of Antennapedia homeodomain and a phospholipid monolayer, studied by ellipsometry and PM-IRRAS at the air−water interface, *Biochim. Biophys. Acta-Biomembr. 1467*, 131−143.
24. Fragneto, G., Graner, F., Charitat, T., Dubos, P., and Bellet-Amalric, E. (2000) Interaction of the third helix of Antennapedia homeodomain with a deposited phospholipid bilayer: A neutron reflectivity structural study, *Langmuir 16*, 4581−4588.
25. Lundberg, M., and Johansson, M. (2002) Positively charged DNA-binding proteins cause apparent cell membrane translocation, *Biochem. Biophys. Res. Commun. 291*, 367−371.
26. Richard, J. P., Melikov, K., Vives, E., Ramos, C., Verbeure, B., Gait, M. J., Chernomordik, L. V., and Lebleu, B. (2003) Cell-penetrating peptides. A reevaluation of the mechanism of cellular uptake, *J. Biol. Chem. 278*, 585−590.
27. Thorén, P. E. G., Persson, D., Isakson, P., Goksör, M., Önfelt, A., and Norden, B. (2003) Uptake of analogs of penetratin, Tat-(48−60) and oligoarginine in live cells, *Bichem. Biophys. Res. Commun. 307*, 100−107.
28. Dokka, S., and Rojanasakul, Y. (2000) Novel non-endocytic delivery of antisense oligonucleotides, *Adv. Drug Deliv. Rev. 44*, 35−49.
29. Fischer, P. M., Krausz, E., and Lane, D. P. (2001) Cellular delivery of impermeable effector molecules in the form of conjugates with peptides capable of mediating membrane translocation, *Bioconjugate Chem. 12*, 825−841.
30. Lindsay, M. A. (2002) Peptide-mediated cell delivery: application in protein target validation, *Curr. Opin. Pharmacol. 2*, 587−594.
31. Wadia, J. S., and Dowdy, S. F. (2003) Modulation of cellular function by TAT mediated transduction of full length proteins, *Curr. Protein Peptide Sci. 4*, 97−104.
32. Beschiaschvili, G., and Seelig, J. (1990) Peptide binding to lipid bilayers − binding isotherms and zeta- potential of a cyclic somatostatin analog, *Biochemistry 29*, 10995−11000.
33. Wimley, W. C., and White, S. H. (2000) Determining the membrane topology of peptides by fluorescence quenching, *Biochemistry 39*, 161−170.
34. Gill, S. C., and Von Hippel, P. H. (1989) Calculation of protein extinction coefficients from amino acid sequence data, *Anal. Biochem. 182*, 319−326.

35. Chico, D. E., Given, R. L., and Miller, B. T. (2003) Binding of cationic cell-permeable peptides to plastic and glass, *Peptides 24*, 3−9.
36. Mayer, L. D., Hope, M. J., and Cullis, P. R. (1986) Vesicles of variable sizes produced by a rapid extrusion procedure, *Biochim. Biophys. Acta 858*, 161−168.
37. New, R. R. C. (1990) in *Liposomes − A Practical Approach* (New, R. R. C., Ed.) pp 108−109, IRL Press/Oxford University Press, Oxford.
38. Perczel, A., Park, K., and Fasman, G. D. (1992) Analysis of the circular dichroism spectrum of proteins using the convex constraint algorithm − a practical guide, *Anal. Biochem. 203*, 83−93.
39. Eftink, M. R., and Ghiron, C. A. (1976) Fluorescence quenching of indole and model micelle systems, *J. Phys. Chem. 80*, 486-493.
40. De Kroon, A. I. P., Soekarjo, M. W., De Gier, J., and De Kruijff, B. (1990) The role of charge and hydrophobicity in peptide lipid interaction − a comparative study based on tryptophan fluorescence measurements combined with the use of aqueous and hydrophobic quenchers, *Biochemistry 29*, 8229−8240.
41. Lakowicz, J. R. (1983) *Principles of Fluorescence Spectroscopy*, Plenum Press, New York.
42. Eftink, M. R., and Ghiron, C. A. (1981) Fluorescence quenching studies with proteins, *Anal. Biochem. 114*, 199−227.
43. Ladokhin, A. S. (1993) Distribution analysis of membrane penetration by depth dependent fluorescence quenching, *Biophys. J. 64*, A290−A290.
44. Ladokhin, A. S. (1997) Distribution analysis of depth-dependent fluorescence quenching in membranes: a practical guide, *Methods Enzymol. 278*, 462−73.
45. Chattopadhyay, A., and London, E. (1987) Parallax method for direct measurement of membrane penetration depth utilizing fluorescence quenching by spin-labeled phospholipids, *Biochemistry 26*, 39−45.
46. Abrams, F. S., and London, E. (1992) Calibration of the parallax fluorescence quenching method for determination of membrane penetration depth: refinement and comparison of quenching by spin-labeled and brominated lipids, *Biochemistry 31*, 5312−5322.
47. Abrams, F. S., and London, E. (1993) Extension of the parallax analysis of membrane penetration depth to the polar-region of model membranes − use of fluorescence quenching by a spin-label attached to the phospholipid polar headgroup, *Biochemistry 32*, 10826−10831.
48. Ladokhin, A. S. (1999) Evaluation of lipid exposure of tryptophan residues in membrane peptides and proteins, *Anal. Biochem. 276*, 65−71.
49. Ladokhin, A. S. (1999) Analysis of protein and peptide penetration into membranes by depth- dependent fluorescence quenching: theoretical considerations, *Biophys. J. 76*, 946−955.
50. London, E., and Ladokhin, A. S. (2002) Measuring the depth of amino acid residues in membrane-inserted peptides by fluorescence quenching, *Curr. Top. Membr. 52*, 89−115.
51. McIntosh, T. J., and Holloway, P. W. (1987) Determination of the depth of bromine atoms in bilayers formed from bromolipid probes, *Biochemistry 26*, 1783−1788.
52. East, J. M., and Lee, A. G. (1982) Lipid selectivity of the calcium and magnesium ion dependent Adenosine-Triphosphatase, studied with fluorescence quenching by a brominated phospholipid, *Biochemistry 21*, 4144−4151.
53. Wiener, M. C., and White, S. H. (1992) Structure of a fluid dioleoylphosphatidylcholine bilayer determined by joint refinement of X-ray and neutron diffraction data. 3. Complete structure, *Biophys. J. 61*, 434−447.
54. Criado, M., and Keller, B. U. (1987) A membrane-fusion strategy for single-channel recordings of membranes usually non-accessible to patch-clamp pipette electrodes, *FEBS Lett. 224*, 172−176.
55. Karlsson, M., Nolkrantz, K., Davidson, M. J., Strömberg, A., Ryttsén, F., Åkerman, B., and Orwar, O. (2000) Electroinjection of colloid particles and biopolymers into single unilamellar liposomes and cells for bioanalytical applications, *Anal. Chem. 72*, 5857−5862.
56. Ladokhin, A. S., Jayasinghe, S., and White, S. H. (2000) How to measure and analyze tryptophan fluorescence in membranes properly, and why bother? *Anal. Biochem. 285*, 235−245.
57. Holland, J. W., Hui, C., Cullis, P. R., and Madden, T. D. (1996) Poly(ethylene glycol)-lipid conjugates regulate the calcium-induced fusion of liposomes composed of phosphatidylethanolamine and phosphatidylserine, *Biochemistry 35*, 2618−2624.
58. Ghosh, A. K., Rukmini, R., and Chattopadhyay, A. (1997) Modulation of tryptophan environment in membrane-bound melittin by negatively charged phospholipids: implications in membrane organization and function, *Biochemistry 36*, 14291−14305.
59. Oren, Z., and Shai, Y. (1997) Selective lysis of bacteria but not mammalian cells by diastereomers of melittin: structure−function study, *Biochemistry 36*, 1826−1835.
60. Ladokhin, A. S., and Holloway, P. W. (1995) Fluorescence of membrane-bound tryptophan octyl ester: a model for studying intrinsic fluorescence of protein-membrane interactions, *Biophys. J. 69*, 506−517.
61. Ziegler, A., Blatter, X. L., Seelig, A., and Seelig, J. (2003) Protein transduction domains of HIV-1 and SIV TAT interact with charged lipid vesicles. Binding mechanism and thermodynamic analysis, *Biochemistry 42*, 9185−9194.
62. Wolber, P. K., and Hudson, B. S. (1979) Analytic solution to the Forster energy-transfer problem in 2 dimensions, *Biophys. J. 28*, 197−210.
63. Hoshiyama, M., Kubo, K., Igarashi, T., and Sakurai, T. (2001) Complexation and proton dissociation behavior of 7-hydroxy-4-methylcoumarin and related compounds in the presence of beta-cyclodextrin, *J. Photochem. Photobiol. A−Chem. 138*, 227−233.
64. Mishra, V. K., Palgunachari, M. N., Segrest, J. P., and Anantharamaiah, G. M. (1994) Interactions of synthetic peptide analogs of the class A amphipathic helix with lipids − evidence for the Snorkel hypothesis, *J. Biol. Chem. 269*, 7185−7191.
65. Clayton, A. H. A., and Sawyer, W. H. (1999) The structure and orientation of class-A amphipathic peptides on a phospholipid bilayer surface, *Eur. Biophys. J. Biophys. Lett. 28*, 133−141.
66. Hristova, K., Wimley, W. C., Mishra, V. K., Anantharamiah, G. M., Segrest, J. P., and White, S. H. (1999) An amphipathic alpha-helix at a membrane interface: A structural study using a novel X-ray diffraction method, *J. Mol. Biol. 290*, 99−117.
67. Gorbenko, G., Saito, H., Molotkovsky, J., Tanaka, M., Egashira, M., Nakano, M., and Handa, T. (2001) Resonance energy transfer study of peptide-lipid complexes, *Biophys. Chem. 92*, 155−68.
68. Seelig, J., Nebel, S., Ganz, P., and Bruns, C. (1993) Electrostatic and nonpolar peptide-membrane interactions − lipid binding and functional properties of somatostatin analogs of charge Z = +1 to Z = +3, *Biochemistry 32*, 9714−9721.
69. Seelig, A., Alt, T., Lotz, S., and Holzemann, G. (1996) Binding of substance P agonists to lipid membranes and to the neurokinin-1 receptor, *Biochemistry 35*, 4365−4374.
70. Wieprecht, T., Apostolov, O., Beyermann, M., and Seelig, J. (1999) Thermodynamics of the alpha-helix-coil transition of amphipathic peptides in a membrane environment: Implications for the peptide-membrane binding equilibrium, *J. Mol. Biol. 294*, 785−794.
71. Breukink, E., Ganz, P., de Kruijff, B., and Seelig, J. (2000) Binding of nisin Z to bilayer vesicles as determined with isothermal titration calorimetry, *Biochemistry 39*, 10247−10254.
72. Eisenberg, M., Gresalfi, T., Riccio, T., and McLaughlin, S. (1979) Adsorption of monovalent cations to bilayer membranes containing negative phospholipids, *Biochemistry 18*, 5213−5223.
73. Schwarz, G., and Beschiaschvili, G. (1989) Thermodynamic and kinetic studies on the association of melittin with a phospholipid bilayer, *Biochim. Biophys. Acta 979*, 82−90.
74. Stankowski, S. (1991) Surface charging by large multivalent molecules − extending the standard Gouy−Chapman treatment, *Biophys. J. 60*, 341−351.
75. Carnie, S., and McLaughlin, S. (1983) Large divalent cations and electrostatic potentials adjacent to membranes. A theoretical calculation, *Biophys. J. 44*, 325−332.
76. Seelig, A., and Macdonald, P. M. (1989) Binding of a neuropeptide, substance P, to neutral and negatively charged lipids, *Biochemistry 28*, 2490−2496.
77. Cantor, C. R., and Schimmel, P. R. (1980) *Biophysical Chemistry*, Vol. 1, W. H. Freeman, San Fransisco.
78. Wimley, W. C., and White, S. H. (1996) Experimentally determined hydrophobicity scale for proteins at membrane interfaces, *Nat. Struct. Biol. 3*, 842−848.
79. Kim, J. Y., Mosior, M., Chung, L. A., Wu, H., and McLaughlin, S. (1991) Binding of peptides with basic residues to membranes containing acidic phospholipids, *Biophys. J. 60*, 135−148.
80. Victor, K. G., and Cafiso, D. S. (2001) Location and dynamics of basic peptides at the membrane interface: Electron paramagnetic resonance spectroscopy of tetramethyl-piperidine-N-oxyl-4-amino-4-carboxylic acid-labeled peptides, *Biophys. J. 81*, 2241−2250.
81. BenTal, N., Honig, B., Peitzsch, R. M., Denisov, G., and McLaughlin, S. (1996) Binding of small basic peptides to

membranes containing acidic lipids: Theoretical models and experimental results, *Biophys. J. 71*, 561−575.
82. Victor, K., Jacob, J., and Cafiso, D. S. (1999) Interactions controlling the membrane binding of basic protein domains: Phenylalanine and the attachment of the myristoylated alanine-rich C-kinase substrate protein to interfaces, *Biochemistry 38*, 12527−12536.
83. Wertz, S. L., Savino, Y., and Cafiso, D. S. (1996) Solution and membrane bound structure of a peptide derived from the protein kinase C substrate domain of neuromodulin, *Biochemistry 35*, 11104−11112.
84. Segrest, J. P., Deloof, H., Dohlman, J. G., Brouillette, C. G., and Anantharamaiah, G. M. (1990) Amphipathic helix motif − classes and properties, *Proteins 8*, 103−117.
85. Mosior, M., and McLaughlin, S. (1992) Binding of basic peptides to acidic lipids in membranes − effects of inserting alanine(s) between the basic residues, *Biochemistry 31*, 1767−1773.
86. Kaznessis, Y. N., Kim, S., and Larson, R. G. (2002) Specific mode of interaction between components of model pulmonary surfactants using computer simulations, *J. Mol. Biol. 322*, 569−582.
87. Batenburg, A. M., Hibbeln, J. C. L., and de Kruijff, B. (1987) Lipid specific penetration of melittin into phospholipid model membranes, *Biochim. Biophys. Acta 903*, 155−165.
88. Yau, W. M., Wimley, W. C., Gawrisch, K., and White, S. H. (1998) The preference of tryptophan for membrane interfaces, *Biochemistry 37*, 14713−14718.
89. Ulmschneider, M. B., and Sansom, M. S. P. (2001) Amino acid distributions in integral membrane protein structures, *Biochim. Biophys. Acta 1512*, 1−14.
90. Landolt-Marticorena, C., Williams, K. A., Deber, C. M., and Reithmeier, R. A. F. (1993) Non-random distribution of amino acids in the transmembrane segments of human type I single span membrane proteins, *J. Mol. Biol. 229*, 602−608.
91. von Heijne, G. (1994) Membrane proteins: from sequence to structure, *Annu. Rev. Biophys. Biomol. Struct. 23*, 167−192.
92. Mall, S., Sharma, R. P., East, J. M., and Lee, A. G. (1998) Lipid−protein interactions in the membrane: Studies with model peptides, *Faraday Discuss.*, 127−136.
93. Johnson, J. E., and Cornell, R. B. (1994) Membrane-binding amphipathic alpha-helical peptide derived from CTP:phosphocholine cytidylyltransferase, *Biochemistry 33*, 4327−4335.
94. Mangavel, C., Maget-Dana, R., Tauc, P., Brochon, J. C., Sy, D., and Reynaud, J. A. (1998) Structural investigations of basic amphipathic model peptides in the presence of lipid vesicles studied by circular dichroism, fluorescence, monolayer and modeling, *Biochim. Biophys. Acta 1371*, 265−283.
95. Hong, J., Oren, Z., and Shai, Y. (1999) Structure and organization of hemolytic and nonhemolytic diastereomers of antimicrobial peptides in membranes, *Biochemistry 38*, 16963−16973.
96. Voglino, L., Simon, S. A., and McIntosh, T. J. (1999) Orientation of LamB signal peptides in bilayers: Influence of lipid probes on peptide binding and interpretation of fluorescence quenching data, *Biochemistry 38*, 7509−7516.
97. Breukink, E., van Kraaij, C., van Dalen, A., Demel, R. A., Siezen, R. J., de Kruijff, B., and Kuipers, O. P. (1998) The orientation of nisin in membranes, *Biochemistry 37*, 8153−8162.
98. Ren, J. H., Lew, S., Wang, Z. W., and London, E. (1997) Transmembrane orientation of hydrophobic alpha-helices is regulated both by the relationship of helix length to bilayer thickness and by the cholesterol concentration, *Biochemistry 36*, 10213−10220.
99. Matsuzaki, K., Murase, O., Fujii, N., and Miyajima, K. (1995) Translocation of a channel-forming antimicrobial peptide, magainin 2, across lipid bilayers by forming a pore, *Biochemistry 34*, 6521−6526.
100. Matsuzaki, K., Yoneyama, S., and Miyajima, K. (1997) Pore formation and translocation of melittin, *Biophys. J. 73*, 831−838.
101. Fischer, A., Oberholzer, T., and Luisi, P. L. (2000) Giant vesicles as models to study the interactions between membranes and proteins, *Biochim. Biophys. Acta 1467*, 177−188.
102. Liu, Y., Jones, M., Hingtgen, C. M., Bu, G., Laribee, N., Tanzi, R. E., Moir, R. D., Nath, A., and He, J. J. (2000) Uptake of HIV-1 tat protein mediated by low-density lipoprotein receptor-related protein disrupts the neuronal metabolic balance of the receptor ligands, *Nat. Med. 6*, 1380−1387.
103. Tyagi, M., Rusnati, M., Presta, M., and Giacca, M. (2001) Internalization of HIV-1 tat requires cell surface heparan sulfate proteoglycans, *J. Biol. Chem. 276*, 3254−3261.
104. Lawson, C. L., and Hanson, R. J. (1974) *Solving Least Squares Problems*, Prentice-Hall, NJ.

BI0360049